UNIVERSIDADE D
COIMBRA

Guilherme Borlido de Carvalho Farias

PHENOTYPING CIRCULATING MONOCYTES AND DENDRITIC CELLS IN SARS-COV-2 AND HIV INFECTIONS

UNSUPERVISED AND SUPERVISED APPROACHES TO FLOW CYTOMETRY DATA ANALYSIS

VOLUME 1

Dissertação no âmbito do Mestrado em Investigação Biomédica com especialização em Infeção e Imunidade orientada pela Doutora Amelia Chiara Trombetta e apresentada à Faculdade de Medicina de Coimbra

Outubro de 2021

Faculdade de Medicina da Universidade de Coimbra

UNIVERSIDADE D
COIMBRA

Guilherme Borlido de Carvalho Farias

PHENOTYPING CIRCULATING MONOCYTES AND DENDRITIC CELLS IN SARS-COV-2 AND HIV INFECTIONS

UNSUPERVISED AND SUPERVISED APPROACHES TO FLOW CYTOMETRY DATA ANALYSIS

VOLUME 1

Trabalho com orientação científica das Doutoras Joana Barbosa de Melo da Faculdade de Medicina de Coimbra e Amelia Chiara Trombetta do Instituto de Medicina Molecular João Lobo Antunes

Outubro de 2021

Abstract

Monocytes and dendritic cells (DCs) are crucial in the response to viral infections, starting and coordinating the inflammatory response and also activating the adaptive immune system components, subsequently having a determinant role in disease outcome. This work utilizes unsupervised and supervised approaches for flow cytometry data analysis, characterizing circulating monocyte and DC phenotype in patients infected by Severe Acute Respiratory Syndrome Coronavirus 2 (SARS-CoV-2) and Human Immunodeficiency Virus (HIV).

SARS-CoV-2 infection, the etiological agent of Coronavirus Disease 2019 (COVID-19), can lead to rampant inflammatory response. Cytokine storm in COVID-19 worsens clinical symptoms. Patients developing severe disease have high case-fatality and require admission to intensive care units and respiratory support. Therefore, severe COVID-19 patients became the bottleneck for the management of the pandemic. Firstly, the aim of the present study was to profile circulating monocytes and DCs in the recovery of patients surviving severe COVID−19. We revealed that the cell phenotype at discharge was characterized by increased immunomodulatory marker expression and accompanied by persistently high levels of immune regulatory cytokines.

Another focus was acute HIV-1 infection. HIV-1 causes a chronic inflammation, progressively dysregulating the immune system responses. Early infection events are thought to be determinant for disease progression. However, data on these stages are scarce for the lack of clinical manifestations, causing difficulties in early detection. We studied the phenotype of circulating monocytes and DCs in an acute HIV-1 patient in comparison to a cohort of SARS-CoV-2 infected patients. In this new analysis, we revealed that $Slan^+$ non-classical monocyte depletion was shared by both acute infections.

Finally, the flow-cytometry panel was expanded, taking advantage of a state-of-the-art spectral flow cytometer, testing it on two chronic HIV-2 patients. HIV-2 displays an attenuated disease without treatment compared to HIV-1. The new panel allowed to assess the phenotype of circulating monocytes and dendritic cells.

Keywords: Monocytes; Dendritic cells; HIV; SARS-CoV-2; Flow cytometry

Resumo

Monócitos e células dendríticas (CDs) coordenam a reposta inflamatória e ativam o ramo adaptativo do sistema imune, sendo fundamentais na resposta a infeções virais. Este trabalho utiliza abordagens automatizadas e manuais na análise de dados de citometria de fluxo para caracterizar o fenótipo dos monócitos e CDs em doentes infetados pelo Vírus da Imunodeficiência Humana (VIH) e Síndrome Respiratória Aguda Grave Coronavírus 2 (SARS−CoV−2).

SARS−CoV−2 causa doença do coronavírus 2019 (COVID-19), que em casos graves leva a uma forte resposta inflamatória. Doentes com COVID-19 grave requerem internamento nos cuidados intensivos. A gestão de recursos de saúde associada a estes é um dos problemas principais desta pandemia. O primeiro objetivo deste estudo foi caracterizar o fenótipo de monócito e CDs durante a recuperação de COVID-19 grave. Ao fazê-lo revelámos que a recuperação de COVID-19 foi associada a um fenótipo imuno-modulatório acompanhado pela manutenção de níveis elevados de citocinas regulatórias.

Outro foco foi o estádio inicial da infeção por VIH-1, que causa uma infeção vitalícia com crescente desregulação do sistema imune. Estes estádios inicias são difíceis de estudar, uma vez que a maioria dos doentes são assintomáticos durante as mesmas. No entanto, estes eventos são determinísticos na progressão da doença. Sendo assim, aproveitamos a oportunidade para estudar o fenótipo destas células numa doente no estádio agudo da infeção por VIH e compará-la a uma coorte de doentes com infeção de SARS-CoV-2 aguda. Este estudo revelou que a perda dos monócitos não clássicos $Slan^+$ era comum a ambas as infeções.

Por fim, expandimos o painel de citometria de fluxo, tirando proveito da tecnologia de citometria de fluxo espectral, e testando-o em dois doentes crónicos infetados VIH−2 em tratamento, um vírus com uma doença atenuada comparado a VIH-1. Este novo painel permitiu a caracterização de monócitos e CDs circulantes com análises automatizadas e manuais.

Palavras-chave: Monócitos; Células dendríticas; VIH; SARS-CoV-2; Citometria de fluxo

Acknowledgments

A special thanks to the Faculdade de Medicina for the time during my master's degree. Professor Henrique Girão work and passion for MIB is admirable and made my time living in Coimbra a wonder.

I would like to tank Ana Espada de Sousa and the rest of the research group for taking me in, guiding me and helping me grow as a researcher. The support of the team was crucial for the realization of the work and it would be correct of me not thank them.

Within the team, I must give a very special thanks to my supervisor, Amelia Trombetta. Her guidance and her availably to help me and to calm me made such a difference in the quality of the work I did that I cannot imagine having a better supervisor. Thank you for an incredible person.

To my family and friends who have always supported me: Thanks!

And to Cláudia, my girlfriend and my best friend, thank you for always being there for me. I honestly don't know if I could finish this without your support. There is much more I could say to thank you, but you already know how much you mean to me.

Table of Contents

List of Abbreviations

AIDS	Acquired Immune Deficiency Syndrome
APC	Allophycocyanin
ARDS	Acute Severe Respiratory Syndrome
Az	Azide
BSA	Bovine serum albumin
BV	Brilliant Violet
CCL	Chemokine (C-C motif) Ligand 2
CCR	Chemokine (C-C motif) Receptor 2
CD	Cluster of differentiation
COVID-19	Coronavirus Disease 2019
CRP	C-reactive protein
CX_3CR	Chemokine (C-X_3-C motif) Receptor
CXCL	Chemokine (C-X-C motif) Ligand
DC	Dendritic Cells
ddPCR	digital droplet Polymerase Chain Reaction
EDTA	Ethylenediamine tetraacetic acid
FcγR	Fragment Crystallizable Region type γ Receptor
Fitc	Fluorescein isothiocyanate
HC	Healthy Control
HIV-1	Human Immunodeficiency Virus type 1
HIV-2	Human Immunodeficiency Virus type 2
HLA-DR	Human Leukocyte Antigen – DR isotype
ICU	Intensive Care Unit
IFN	Interferon
IL	Interleukin
IL-1RA	Interleukin-1 Receptor Antagonist
IL-22BP	Interleukin 22 Binding Protein
$KHCO_3$	Potassium Bicarbonate
LDH	Lactate Dehydrogenase
LPS	Lipopolysaccharides
MCP	Monocyte Chemotactic Protein
mDC	Myeloid Dendritic Cells

List of Abbreviations

MIP	Macrophage Inflammatory Protein
MHC	Major Histocompatibility Complex
NH_4Cl	Ammonium Chloride
NHP	Non-Human Primate
NO	Nitric Oxide
PBS	Phosphate Buffered Saline
PCA	Principal Component Analysis
PCR	Polymerase Chain Reaction
pDC	Plasmacytoid Dendritic Cells
PD-L1	Programmed Death Ligand 1
PE	R-Phycoerythrin
PerCP	Peridinin-Chlorophyll-Protein
PPR	Pattern Recognition Receptors
RAGE	Receptor for Advanced Glycation Endproducts
RBC	Red Blood Cells
ROS	Reactive Oxygen Species
RT-PCR	Real Time Polymerase Chain Reaction
SAMHD-1	SAM- and HD-domain- containing protein
SARS-CoV-2	Severe Acute Respiratory Syndrome Coronavirus 2
Slan	6-Sulfo LacNAc
SP-D	Pulmonary Surfactant protein D
TNF	Tumour Necrosis Factor
UMAP	Uniform Manifold Approximation and Projection

List of Figures

List of Supplementary Figures

List of Tables

1. Introduction

1.1. Innate immunity and Viral Infections

The innate immune system is vital in keeping tissue homeostasis and acts as the first line of defence against viral pathogens, playing a critical role in both early and late stages of infection. Many pathogens evolved mechanisms to evade and/or highjack the innate immune system and promote their proliferation. The cells of the innate immune system detect the pathogen through pattern recognition receptors (PPR) and mount the initial inflammatory response, while also activating the adaptive immune response through antigen presentation. In the later phases of the infection, the innate branch works in tandem with the adaptive branch to remove the pathogen and return to homeostasis (Auffray, Sieweke e Geissmann, 2009; Hart, 1997).

Given the importance of the innate immune system cells in all stages of infection, characterizing their phenotype can give crucial insight on the disease course and prognosis. In this study, we investigated the phenotype of two major circulating populations in the innate immune system: monocytes and dendritic cells. Their profile was studied in the context of two viral infections, Severe Acute Respiratory Syndrome Coronavirus 2 (SARS-CoV-2) and Human Immunodeficiency Virus (HIV) type 1 (HIV-1) and type 2 (HIV-2).

1.2. The Heterogeneity of Blood Monocytes

Monocytes are a population of circulating leukocytes with a major role in the inflammatory response, representing around 10% of circulating leukocytes. Monocytes can quickly leave circulation trough extravasation to the tissue sites of inflammation. They can exert several functions during an immune response, being able to perform phagocytosis, antigen presentation and secrete a variety of cytokines and chemokines. Altogether, monocytes contribute to the coordination of both the innate and adaptive immune response. Another feature of monocytes is their high phenotype plasticity, differentiating into more specialized populations at the tissue level, such as macrophages and dendritic cells (DC) (Auffray, Sieweke e Geissmann, 2009; Ginhoux e Jung, 2014).

In circulation, monocytes are classified into three main subsets based on the expression of CD14, the co-receptor for the LPS and CD16, the Fcγ receptor III: classical monocytes are defined as $CD14^{high}CD16^{-}$, intermediate monocytes as $CD14^{high}$ $CD16^{+}$ and non-classical monocytes as $CD14^{low/-}$ $CD16^{+}$. Monocytes are released from the bone marrow into the circulation as classical monocytes and then differentiate into intermediate monocytes and finally non-classical monocytes in a period of around 10 days (Patel *et al.*, 2017; Rogacev *et al.*, 2015; Tak *et al.*, 2017). This differentiation is accompanied by increasing signs of

senescence (Ong *et al.*, 2018). It is important to note that the variation in the expression of both CD14 and CD16 in human is a continuum and can change significantly under certain conditions such as in diseases (Cignarella *et al.*, 2018; Kapellos *et al.*, 2019). Nevertheless, the different subsets express other surface molecules that correspond to specific transcriptomic profiles, reflecting specialization into different functions (Ong *et al.*, 2019; Patel *et al.*, 2017; Wilk *et al.*, 2020; Wong *et al.*, 2011) (**Figure 1**).

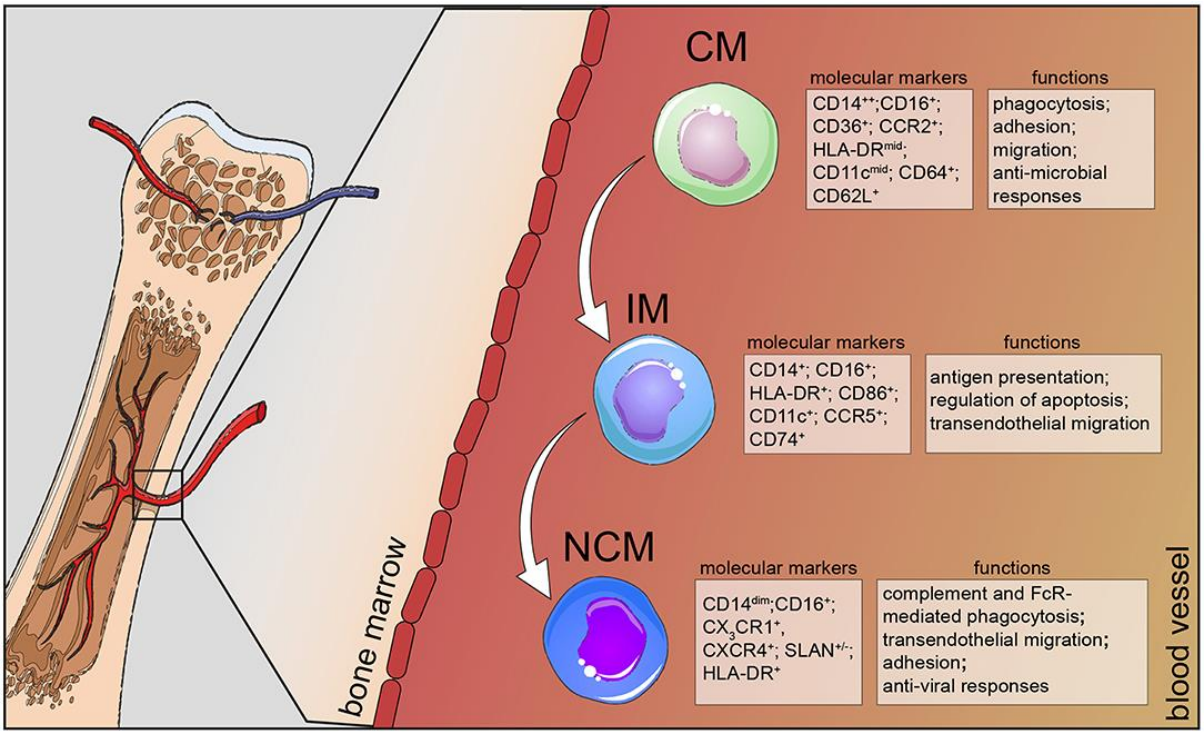

Figure 1 – **Circulating Monocyte Subsets in steady state**.
Monocytes are released into the circulation as classical monocytes. Classical monocytes express also higher levels of CD36, CCR2, and CD64 and take part in anti-microbial responses, such as adhesion to the endothelium, migration, and phagocytosis. Intermediate monocytes have high expression of CCR5, CD86 and HLA-DR and are involved in antigen processing and presentation and trans endothelial migration. Non-classical monocytes can be divided in $SLAN^+$ or $SLAN^-$, both having high expression of CX_3CR1 and are specialized in complement and FcR-mediated phagocytosis, trans-endothelial migration and anti-viral responses. CM, classical monocytes; IM, intermediate monocytes; NCM, non-classical monocytes. Adapted from Kapellos, TS *et al,* Front. Immunol. (2019) doi: 10.3389/fimmu.2019.02035

Classical monocytes are the main population, representing 85-90% of all monocytes in circulation. Transcriptomic data showed that classical monocytes have high phagocytic capacity and express a variety of innate sensing receptors. This subset expresses the highest levels of the chemokine (C-C motif) receptor 2 (CCR2), showing high sensitivity for its ligand CCL2 (Thiesen *et al.*, 2014). The expression of CCR2 together with other chemokine receptors and the secretion of cytokines such as interleukin 6 (IL-6), IL-1β, tumour necrosis factor α (TNF-α) and IL-10 reflects their ability to be recruited to the sites of inflammation and be key players in the coordination of the immune response. Intermediate monocytes express the highest levels of human leukocyte antigen – DR isotype (HLA-DR) and the co-stimulatory ligand CD86 in circulation, which indicates their enhanced ability for antigen presentation and

stimulation of T-cells (Gren *et al.*, 2015; Wong *et al.*, 2011). This subset and the non-classical subset also express immune modulatory molecules such as the programmed death ligand 1 (PD-L1) (Bianchini *et al.*, 2019).

Non-classical monocytes are known for their “patrolling” behaviour that was first described in murine models. The patrolling behaviour can be observed when they adhere to the blood vessel endothelium and move against blood circulation (Auffray *et al.*, 2007). In humans, non-classical monocytes seem to have a more pro-inflammatory profile. Their rapid extravasation is mediated by a high expression of the Fractalkine receptor (CX_3CR1) (Ancuta *et al.*, 2003), which is associated to their activation and survival (Landsman *et al.*, 2009). Another characteristic of the non-classical monocyte population is the ability, compared to other subsets, to produce higher amounts of pro-inflammatory molecules, such as TNF-α and IL-1β after stimulation (Chimen *et al.*, 2017; Wong *et al.*, 2011). Non-classical monocytes can be divided further divided into two populations based on the expression of the 6-Sulfo LacNAc (Slan) (Hofer *et al.*, 2019; Micheletti *et al.*, 2016; Schäkel *et al.*, 2002; Wong *et al.*, 2011). The $Slan^+$ subset produces the highest amounts of TNF-α, IL-1β and IL-12. After extravasation, $Slan^+$ monocytes can display a DC like phenotype with capacity to co-stimulate $CD4^+$ T-cells (Micheletti *et al.*, 2016; Schäkel *et al.*, 2002, 2006) and are expanded in chronic inflammation (Hänsel *et al.*, 2011; Thomas *et al.*, 2014).

1.3. M1 vs M2 Phenotype

The monocyte/macrophage system is essential in maintaining the homeostasis during steady state by performing functions such as debris clearance, secretion of extracellular matrix precursors and downregulation of the immune response. In fact, monocyte/macrophage phenotype is highly plastic and reflects a myriad of signals received from the environment and consequently it is described as a spectrum with defined extremes, with a single cell often showing markers of both sides (Kratz *et al.*, 2014; Mosser e Edwards, 2008; Piccolo *et al.*, 2017; Xue *et al.*, 2014).

One extreme of this polarization is constituted by “classically activated” or M1-like phenotype, these cells being characterized by the production of pro-inflammatory cytokines of the type 1 response, reactive oxygen species (ROS) and nitric oxide (NO). The M1 differentiation is characterized by the expression of the co-stimulatory ligands CD80 and CD86, and the antigen presenting molecule HLA-DR (Elgueta *et al.*, 2009; Gordon, 2003; Mosser e Edwards, 2008; Subauste, Waal Malefyt, de e Fuh, 1998).

On the other extreme of the spectrum there is the “alternatively activated” or M2-like phenotype, encompassing several subclasses that result from different specific stimulations leading to specialization into several functions, such as debris clearance, type 2 response, wound healing and immune regulation (M2a, M2b, M2c and M2d). Although the surface

markers expressed vary within each M2 subclass, canonical surface markers of the more immunomodulatory phenotype are the scavenger receptor for the haemoglobin-haptoglobin complex (CD163), the macrophage class A scavenger receptor (CD204) and the mannose scavenger receptor (CD206), producing several immunomodulatory cytokines (Gordon, 2003; Gordon e Martinez, 2010; Kubota *et al.*, 2017; Varin *et al.*, 2010).

1.4. Dendritic Cell subsets and Functions in Immune Response

Dendritic cells are highly specialized in antigen presentation and are essential in connecting the innate and the adaptive immune response (Hart, 1997). Several subtypes of dendritic cells have been identified in blood. The two main subsets are the plasmacytoid dendritic cells (pDCs) and the conventional or myeloid dendritic cells (mDCs), with the last one being further classified based on their expression of either thrombomodulin (CD141) or the MHC-like CD1 C (CD1c) (Alculumbre *et al.*, 2019; Bachem *et al.*, 2010; Crozat *et al.*, 2010; Jongbloed *et al.*, 2010; Liu, 2005; MacDonald *et al.*, 2002; Schultze e Aschenbrenner, 2019).

Plasmacytoid DCs are known for their high and rapid production of type I interferons after stimulation. This, together with their expression of several intracellular toll-like receptors that recognize components of viral pathogens makes them a key player in the immune response to viral infections, especially in the acute phases. These cells can be identified in circulation by their expression of HLA-DR and the α chain of the IL-3 receptor (CD123) (Alculumbre *et al.*, 2019; Liu, 2005). Myeloid DCs expressing CD1c ($CD1c^+$ mDCs) are the main dendritic cell population found in circulation and are more specialized in the antigen presentation and stimulation of naïve $CD4^+$ T-cells, while $CD141^+$ mDC stimulate more effectively $CD8^+$ T-cells (Bachem *et al.*, 2010; Crozat *et al.*, 2010; Jongbloed *et al.*, 2010; MacDonald *et al.*, 2002; Schultze e Aschenbrenner, 2019).

1.5. SARS-CoV-2 Infection Effects on circulating Monocytes and DCs

After its outbreak in late 2019 from Wuhan, China, the coronavirus disease 2019 (COVID-19), caused by the severe acute respiratory syndrome coronavirus 2 (SARS-CoV-2) infected and killed millions worldwide, having a substantial economic and social impact (Huang *et al.*, 2020). Most infected individuals show mild symptoms with a flu-like syndrome accompanied by respiratory impairment. However, the 5% of cases develop severe disease, in which the rapid viral replication accompanied by a dysregulated immune response leads to Acute respiratory distress syndrome (ARDS), multi-organ failure and a high mortality rate (Guan *et al.*, 2020; Huang *et al.*, 2020). Severe COVID-19 has a higher incidence in certain risk groups (Naveed *et al.*, 2021) and represents the bottleneck of the pandemic management due to the saturation of health care resources. In the absence of an effective treatment for

severe cases, understanding the changes in the immune system can help guide new therapeutics an directing more efficiently the limited health resources.

The main pathogenic event associated with worse prognosis in COVID-19 is the cytokine storm or monocyte/macrophage activation syndrome. In this context, high amounts of pro-inflammatory cytokines, such as IL-6, IL-18, IL-1β, TNF-α and IFN-γ, are secreted. A parallel production of immune modulatory cytokines, such as IL-10 and interleukin-1 receptor antagonist (IL-1RA), is observed (Fajgenbaum e June, 2020; Haljasmägi *et al.*, 2020; Lee *et al.*, 2020; Silvin *et al.*, 2020).

The cytokine storm is accompanied by significant alterations in both frequency and phenotype of monocytes, macrophages and dendritic cells. Circulating cell populations have been shown to be reduced, altered in phenotype or in subset frequencies. Also, an impaired production of cytokines was reported (Zhou *et al.*, 2020). Monocytes in particular were shown to have altered subset frequencies and phenotype, with studies reporting the expression markers from both M1 and M2 (Schulte-Schrepping *et al.*, 2020; Silvin *et al.*, 2020; Valle, Del *et al.*, 2020; Zhang *et al.*, 2021; Zingaropoli *et al.*, 2021).

1.6. HIV-1 Effects in Circulating Monocytes and Dendritic Cells

According to the World Health Organization, in 2020 there were 37.7 million people living with human immunodeficiency virus type 1 (HIV-1), with 1.5 million of those being new infections. HIV-1 causes a life-long infection that leads to a decline in $CD4^+$ T-cells, determining the onset of acquired immune deficiency syndrome (AIDS). The establishment of anti-retroviral therapy (ART) has proven to be the key for infection control, however no definitive cure and effective vaccine are currently available. In fact, those under ART have low to undetectable viremia, preventing transmission, and most maintain $CD4^+$ T-cells counts close to normal values. However, ART constitutes a lifelong treatment, as the virus integrates into the host cell genome, creating viral reservoirs that restart the viral replication if treatment is interrupted. Despite the life expectancy of infected patients becoming closer to non-infected individuals, the incidence of co-morbidities is higher and starts earlier (Marcus *et al.*, 2020). The earlier incidence of co-morbidities normally associated with aging is thought to be caused by chronic immune activation and inflammation (Bahrami *et al.*, 2016; Triant *et al.*, 2007).

HIV-1 infection pathogenesis can be divided into two phases: an early acute phase and a chronic phase (**Figure 2**). In both, the innate immune system plays a key role in pathogenesis and disease prognosis.

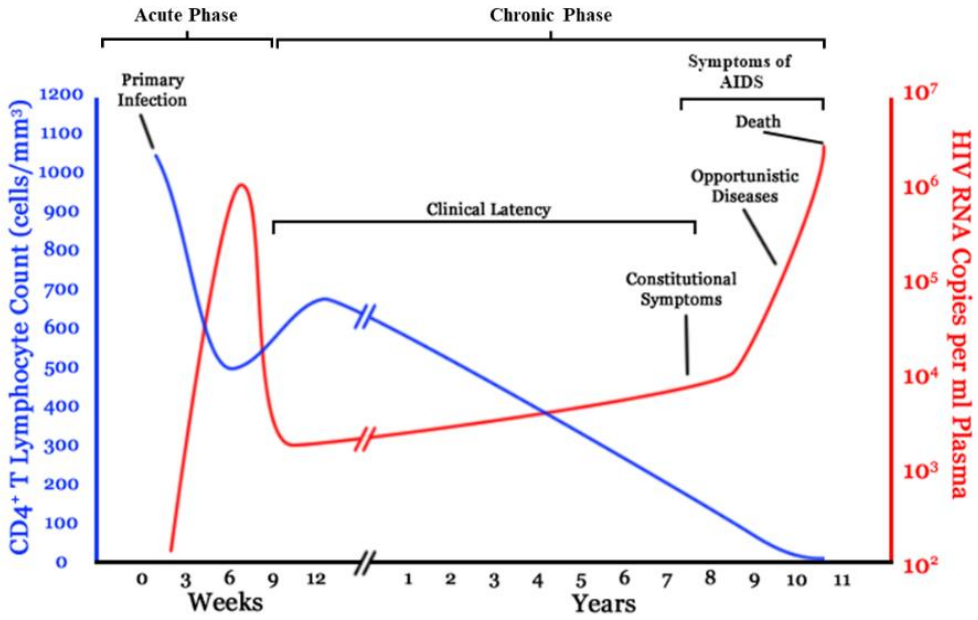

Figure 2 – **Typical course of HIV-1 infection.**
Adapted from Epstein, FH.*et al,* N Engl J Med (1993) doi: 10.1056/NEJM199302043280508

Studies on the acute phase are difficult since most patients are asymptomatic during this stage and will only show symptoms in the chronic phase, with the onset of AIDS (Vanhems *et al.*, 1998). Therefore, most studies on the acute phase come from the non-human primate models (NHP) or from few longitudinal studies performed on uninfected persons in areas of high HIV–1 incidence. Nevertheless, the events that occur during this stage affect the progression of the disease in the chronic stage and start of ART at this stage is associated with better disease control (Jain *et al.*, 2013).

Monocytes and dendritic cells are recognized as key players in the acute HIV infection, due to their role in coordinating the inflammatory response and in activating the adaptive branch of the immune system. Active $CD4^+$ T-cells are the main targets of the virus and $CD8^+$ T-cells responses are among the main contributors to the initial decrease in viremia and establishment of the viral set point, initiating the chronic stage of the infection (Cockerham *et al.*, 2014; Costa *et al.*, 2001; Lécuroux *et al.*, 2009). However, data on the phenotype of monocytes and DCs in the acute stage of infection are relatively scarce. Monocytes seem to show an upregulation of markers like HLA-DR (Kazer *et al.*, 2020; Liu *et al.*, 2019; Novelli *et al.*, 2020). The activation of monocytes coincides with the increase of pro-inflammatory mediator molecules, like CCL2 and IFN-γ, that accompany the rise to peek viremia (Muema *et al.*, 2020). Dendritic cells also play an important role in the early response. As specialized antigen presenting cells, they are essential for adaptive immune system activation and viral dissemination. pDC are among the earliest producers of interferons and are determinant for the start the anti-viral response (O'Brien, Manches e Bhardwaj, 2012).

The activation of monocytes and DCs is maintained throughout the chronic phase of infection, with the pro-inflammatory state being an hallmark of chronic HIV-1 infection, that is exacerbated with the onset of AIDS (Bahrami *et al.*, 2016). In chronic HIV-1 infected individuals, increased frequencies of circulating non-classical monocytes, increased expression of activation markers in monocytes (Chen *et al.*, 2017; Covino *et al.*, 2020; Novelli *et al.*, 2020; Thieblemont *et al.*, 1995) and anti-apoptosis signals (Giri *et al.*, 2009) were described. On the other hand, DCs are diminished in chronically infected patients, but show upregulation of activation markers (Grassi *et al.*, 1999).

As mentioned before, the pro-inflammatory state in monocytes and DCs is maintained even after the start of ART, possibly contributing to the incidence of co-morbidities (Cavaleiro *et al.*, 2013; Novelli *et al.*, 2020). Characterizing myeloid cell phenotypes could help creating strategies to reduce the impact of chronic inflammation on the quality of life of people living with HIV-1 and increase the effectiveness of the treatment.

1.7. HIV-2, an Attenuated Form of HIV-1

HIV-2 is a lentivirus with many similarities to HIV-1, however most of the infected individuals show low to undetectable viremia and relatively stable levels of $CD4^+$ T-cells, declining at a much slower rate when compared to HIV-1 infection (Azevedo-Pereira e Santos-Costa, 2016). With a lower transmission rate, its dissemination is limited to mainly to West Africa and historically connected countries, such as Portugal and France (Carvalho *et al.*, 2012). Similarly to HIV-1 infection, a pattern of chronic inflammation also characterizes HIV-2 pathogenesis, even in patients under ART (Cavaleiro *et al.*, 2013).

Interestingly, one of the main differences between HIV-1 and HIV-2 is the presence of the vpx protein gene in the HIV-2 genome. Vpx promotes the degradation of the endogenous restriction factor SAM- and HD-domain- containing protein (SAMHD-1), an enzyme the phosphohydrolases deoxynucleotides triphosphate into 2'-deoxynucleotides and phosphate in the cytosol. Decreasing the cytosolic concentrations of deoxynucleotides triphosphate hinder the reverse transcription of the viral DNA. SAMHD-1 is expressed at high levels in monocytes, macrophages and dendritic cells, making them non-permissive to HIV-1 infections (Laguette *et al.*, 2011) and its expression is increased by IFN-γ (Li, Zhang e Cao, 2000).

Studies on the immune activation dynamics that determine the differential course in HIV-2 infected patients may elucidate important pathogenic mechanisms and possibly unveil new therapeutic objectives against AIDS development.

1.8. Aims of the Study

The aim of the study was to characterize the phenotypes changes of circulating monocyte and dendritic cell populations in SARS-CoV-2 and HIV in order to elucidate their role in the immune response.

The first aim of the study was the evaluation of phenotypic changes in circulating monocytes and DCs that occurred during severe COVID-19 recovery in patients admitted to the ICU (ICU group) versus patients that did not require ICU admission (No-ICU group) compared to age and sex matched healthy controls. To achieve this, we used both unsupervised and supervised analysis of flow cytometry data and associated them with clinical data, such as disease severity parameters and outcome. The phenotype modifications found in affected patients also correlated with viremia levels and several serum cytokine and chemokine concentrations. The results of this study resulted in a publication in Frontiers Immunology (Trombetta *et al.*, 2021).

The secondary aim of the study was the evaluation of the circulating monocyte and DC phenotype in acute HIV-1 infection. We had the opportunity to study a recently infected HIV-1 patient still in the acute stage and compared the phenotype of its circulating monocytes and DCs to an ART naïve chronically infected individual and to the COVID-19 cohort, in the acute stage of SARS-CoV-2 infection. These new analysis resulted in a short communication that was published in the special edition of Viruses “Transmission and Prevention of HIV: Lessons for the SARS-CoV-2 Pandemic” (Farias *et al.*, 2021).

Also, we were able to expand the flow cytometry panel for the characterization of circulating monocytes and DCs, to achieve a more complete phenotype characterization and take advantage of the potential of spectral flow cytometry. This new flow cytometry panel was then applied to evaluate the circulating cell phenotype of two chronic HIV-2 infected individuals and one healthy control, to assess the phenotype of both monocytes and dendritic cells in treated HIV-2 patients using unsupervised analysis.

2. Material and Methods

2.1. Patients and Controls

HIV-1, HIV-2 and SARS-CoV-2 infected patients were followed at the Centro Hospitalar Universitário Lisboa Norte (CHULN, Lisbon, Portugal). Informed consent was obtained from all participants, and the study was approved by the Ethics committee of the CHULN/Faculdade de Medicina da Universidade de Lisboa/Centro Académico de Medicina de Lisboa. Twenty patients with pneumonia related to COVID-19 and eleven healthy controls (HC), age and sex matched, were enrolled in this study. SARS-CoV-2 infection was confirmed by real-time PCR (RT-PCR) of nasopharyngeal swabs.

Clinical evaluation and blood sampling was performed on patients requiring ICU admission and respiratory support (ICU group) and patients that did not require respiratory support nor ICU admission (No-ICU group). Afterwards, all patients were evaluated at discharge from hospital or ICU.

This project also included two HIV-1 infected patients, one individual in the acute stages of infection and one in the chronic stages of infection. The acute HIV-1 patient was a 22-year-old female at Fiebig stage II (Fiebig *et al.*, 2003). The chronic HIV-1 patient was 49-year-old male not previously exposed to antiretroviral therapy.

Finally, two chronic HIV-2 patients under ART were enrolled for the testing of an expanded flow cytometry panel, a 70-year-old female and a 72-year-old male.

2.2. Whole Blood Sample Processing and Flow Cytometry

Whole blood was processed immediately after sampling and there was no difference in sample handling between patients and control. The whole blood was collected into S-Monovette® EDTA tubes (SARSTEDT, Munich, Germany). The tubes were centrifuged at 800g for 10 min to separate the plasma from the cellular components of the blood. The plasma was colleted and stored at -80ºC, while the plasma volume was replaced by the same volume of PBS/BSA/Az (Bovine serum albumin 2.5g/L, Azide $5x10^{-4}$ µM). Erythrocytes were lysed by incubating the samples in a volume ratio of 1:25 with Bulk Lysis buffer (NH_4Cl 155 mM, $KHCO_3$ 100 mM, EDTA 1 mM, pH 7.4) for 15 minutes at room temperature. Ten million cells were then incubated with FcR block (Miltenyi Biotec, Cologne, Germany) for 30 min at 4ºC. After, samples were incubated at room temperature for 30 minutes with either the conventional cytometry panel (**Table 1**) or the spectral flow cytometry panel (**Table 2**).

Table 1 **– Conventional flow cytometry surface staining panel**

Antibody	Fluorochrome	Clone	Source
Slan	VioBlue	DD-1	Milteny Biotec
CD141	BV510	1A4	BD Biosciences/BD Horizon
CD45	BV605	HI30	BD Biosciences
HLA-DR	BV650	L243	Biolegend
CD86	BV711	IT2.2	Biolegend
PD-L1	BV785	29E2A3	Biolegend
CD3	Fitc	αT3	eBioscience/Invitrogen
CD19	Fitc	HB19	eBioscience/Invitrogen
CD66b	Fitc	G10FS	Biolegend
CD14	PerCP Cy5.5	61D3	eBioscience/Invitrogen
CD80	PE	2D10	Biolegend
CD163	Pe Dazzle-594	GH1/61	Biolegend
CD206	Pe-Cy5	15-2	Biolegend
CD123	Pe-Cy7	6H6	eBioscience
CD204	APC	7C9C20	Biolegend
CD16	Af700	368	Biolegend
CD1c	APC-Cy7	L161	Biolegend

Table 2 - **Spectral flow cytometry surface staining panel**

Antibody	Fluorochrome	Clone	Source
CD3	BV421	SK7	Biolegend
CD19	BV421	HIB19	BioLegend
CD66b	BV421	6/40c	BioLegend
Slan	VioBlue	DD-1	Milteny Biotec
CD141	BV510	1A4	BD Biosciences/BD Horizon
CCR2	BV605	K036C2	Biolegend
HLA-DR	BV650	L243	Biolegend
CD86	BV711	IT2.2	Biolegend
PD-L1	BV785	29E2A3	Biolegend
CD45	Af532	HI30	eBioscience/Invitrogen
CX3CR1	PerCP eflour710	2A9-1	eBioscience/Invitrogen
CD14	PerCP Cy5.5	61D3	eBioscience/Invitrogen
CD33	PE	P67.6	BD Biosciences/BD Horizon
CD163	Pe Dazzle-594	GH1/61	Biolegend
CD206	Pe-Cy5	15-2	Biolegend
CD123	Pe-Cy7	6H6	eBioscience
CD204	APC	7C9C20	Biolegend
CD16	Af700	368	Biolegend
CD1c	APC-Cy7	L161	Biolegend

When surface staining was performed, the cells were fixated with FACS lysing solution (1/10 dilution in dH_2O of FACS Lysing Solution Concentrate, BD Biosciences, Franklin Lakes, NJ, USA) and then resuspended in PBS/BSA/Az and acquired in either a Fortessa X20 (BD

Biosciences) conventional flow cytometer or in a Cytek Aurora (Cytek, Amsterdam, Netherlands) spectral flow cytometer.

When an intracellular staining was performed, the surface-stained samples were processed following the instructions of the eBioscience™ Transcription Factor Staining Buffer Set from Thermofisher (Waltham, MA, USA). Samples were incubated for 10 min at room temperature with 1X RBC Lysis Buffer, washed and then incubated for 30 min at 4ºC with Fixation/Permeabilization Buffer (1/4 mixture of Fixation/Permeabilization Buffer concentrate and Fixation/Permeabilization Diluent). Then staining was performed for 30 min at 4ºC with the intracellular antibodies. In this study, the only intracellular antibody used was anti–SAMHD–1, which was obtained as unconjugated (clone I19-18, Merck, Darmstadt, Alemanha) and conjugated with Fitc at the facilities in Instituto Gulbenkian para Ciência (Oeiras, Portugal). Finally, the cells were resuspended in PBS/BSA/Az and acquired either in a conventional flow cytometer Fortessa X20 (BD Biosciences) or in a spectral flow cytometer Cytek Aurora.

2.3. Unsupervised Analysis

To evaluate the profile of monocytes and DCs in severe COVID-19 recovery, the same number of events from the $CD45^{+}Lin^{-}$ gate were analysed from each patient and HC samples and dimensionality reduction was performed on the dataset using Uniform Manifold Approximation and Projection (UMAP) (McInnes, Healy e Melville, 2018). For clustering, the X-shift algorithm was used (Samusik *et al.*, 2016). This analysis was made in FlowJo v10.7 (Tree Star Inc., Ashland, OR, USA) using the plugins *XShift* v1.4.1 and *UMAP* v3.1.

For the evaluation of the monocyte profile in acute SARS-CoV-2 and HIV-1 and to describe the phenotype in two chronic HIV-2 patients, the workflow described by Melsen J. et al [29] was followed. After compensation in FlowJo v10.7, the $CD45^{+}Lin^{-}$ cells were selected, including the same number of events from each patient and healthy control. The data were transformed and normalized in R v4.1.0 with Bioconductor v3.13 (Huber *et al.*, 2015), then UMAP was applied using the *uwot* package. For clustering of the dataset, the X-shift algorithm was applied to define the appropriate number of clusters for the dataset. Afterwards, the data were clustered using FlowSOM (Gassen, Van *et al.*, 2015) with the defined number of clusters being generated.

2.4. HIV-1 and HIV-2 Read-outs

Plasma viral load was measured on whole blood in EDTA by RT-PCR, in a Cobas 6800/8000® (Roche, Basel, Switzerland), targeting the LTR and gag regions of HIV-1 and HIV-2 genome, enabling quantification. Detection of antibodies for HIV-1 and HIV-2, was made using a fourth generation ELISA (Cobas 8000; Roche, Basel, Switzerland). Antigenemia for

p24 was measured using Evolis system (BioRad; Hercules, CA, USA). Finally, western blots were performed on Env, Pol and Gag for HIV-1 and 2, NewLavBlot 1 and NewLavBlot 2 assays in a Autoblot 3000 (BioRad).

2.5. SARS-Cov2 Plasma Viral Load

To quantify SARS-Cov2 plasma viral load, a digital droplet PCR (ddPCR) was performed using the SARS-CoV-2 ddPCR Test Kit (Bio-Rad), according to manufacturer instructions, on a QX200™ ddPCR System (Bio-Rad). RNA was extracted from 560 µL of plasma using the QIAamp® Viral-RNA MiniKit (QIAGEN, Hilden, Germany), duplicates of 20 µL ddPCR reaction using 5 µL RNA were analysed on QuantaSoft Analysis Pro (1.0.596). Samples were considered viremic when the N1 or N2 regions or both were detected. The viral RNA concentration was calculated in copies per millilitre (cps/mL) according to the extracted volume of plasma.

2.6. Serum Proteins

Serum concentrations of 71 cytokines and chemokines were measured on the plasma stored at −80 ºC using a Multiplexing LASER Bead Assay (Human Cytokine Array/Chemokine Array 71-Plex Panel, HD-71, Eve Technologies, Calgary, Canada). CCL28, RAGE, SP-D and IL-22BP concentrations were measured using Sandwich ELISA kits (RayBiotech, Atlanta, GA, USA), performed according to manufacturer instructions. Principal Component Analysis (PCA) was performed for dimensionality reduction and evaluation of relevant analytes contributing to data variation.

To measure specific antibody responses to SARS-CoV-2, the levels of IgM, IgG, and IgA against spike protein or its receptor binding domain were measured through a quantitative test, as described in (Figueiredo-Campos *et al.*, 2020).

2.7. Statistical Analysis and Data Visualization

Data analysis was performed in R (v4.1.0) and GraphPad Prism version 8 (GraphPad Software, San Diego, CA, USA). Kruskall-Wallis and Dunn's multiple comparison tests were used to compare variables with continuous distribution in more than two groups. Wilcoxon matched-pairs signed rank test was used for paired analysis of continuous data and Mann–Whitney U–test was used for unpaired analyses of continuous data. For hypothesis testing of correlations, Spearman's Delta was done. A p value <0.05 was considered statistically significant. Data visualization was made using the *pheatmap, EnhancedVolcano, ggplot2 and tidyverse* packages for R.

3. Results

3.1. Characterization of Monocytes and Dendritic Cells in Patients Recovering from Severe COVID-19

3.1.1. Characterizing the profile of circulating monocytes and DCs at the recovery stage of severe COVID-19.

To assess the phenotype of circulating monocytes and DCs at recovery from severe COVID-19, data were collected at admission (A) and discharge (D) from patients in the ICU or the respiratory isolation unit (No-ICU group) (**Table 3**).

Table 3 **– Clinical Data and Blood Work from COVID-19 Patients and Healthy Controls**

Clinical variables		No-ICU	ICU	HCs	p (Global)[a]	p (ICU vs HCs)[b]	p (No ICU vs HCs)[b]	p (ICU vs No-ICU)[b]
Number of individuals (n)		9	11	11				
Age in years		50 (39-65)	57 (45.5-64)	58 (39-65)	0.485	0.965	0.965	0.965
Male sex, n (%) [c]		7 (77.7)	10 (91)	9 (73)	0.671	0.315	0.882	0.413
Arterial hypertension, n (%) [c]		4 (44)	5 (46)	1 (9)	0.264	0.056	0.069	0.964
Diabetes type 2, n (%) [c]		3 (33)	3 (27)	0	0.251	0.062	**0.038**	0.2942
Obesity, n (%) [c]		1 (11)	5 (45)	0	**0.032**	**0.011**	0.257	0.095
Lung emphysema. n (%) [c]		0	2 (18)	0	0.313	0.138	>0.999	0.178
Time from symptoms start to admission (days)		8 (4-10)	9 (7-12)	NA	0.302	NA	NA	0.302
Time from symptoms start to recovery (days)		12 (11-17)	20 (17-21.5)	NA	**0.009**	NA	NA	**0.009**
Time from admission to discharge (days)		9 (8-10)	12 (9.5-15)	NA	**0.034**	NA	NA	**0.034**
P/f	A	287.4 (270-323)	122.1(104.5-272.2)	NA	NA	NA	NA	**<0.001**
	D	447.6 (340-461)	283.3 (273-392.9)	NA	NA	NA	NA	**0.03**
CRP (mg/dl)	A	5.44 (2.26-7.03)	23.7 (12.5-26.5)	NA	NA	NA	NA	**0.005**
PCT (ng/ml)	A	0.14 (0.11-0.41)	0.21 (0.15-0.83)	NA	NA	NA	NA	0.440
Ferritin (mg/dl)	A	949 (344-1374)	1030 (435.3-1998)	NA	NA	NA	NA	0.450
D-dimers (ng/ml)	A	0.43 (0.19-53)	0.23 (0.18-0.63)	NA	NA	NA	NA	0.712
LDH (U/l)	A	366 (222-417.5)	372 (293-393)	NA	NA	NA	NA	0.736
Lymphocytes/µl	A	1390 (835-2108)	870 (840-1160)	1940 (1423-2200)	**0.005**	**0.003**	0.152	0.146
	D	1810 (1675-1995)	1982 (1269-2680)		0.8464	0.710	0.661	0.898
Neutrophils/µl	A	3923 (2385-4952)	7447 (4687-11793)	3228 (2521-6390)	**0.011**	**0.010**	0.924	**0.007**
	D	3349 (2792-4891)	5557 (4303-9620)		**0.067**	**0.045**	0.978	**0.**060
Lymphocytes/neutrophils	A	0.316 (0.26-0.65)	0.146 (0.086-0.380)	0.509 (0.47-0.605)	**0.013**	**0.008**	0.194	**0.038**
	D	0.588 (0.35-0.69)	0.264 (0.142-0.559)		0.098	**0.005**	0.892	**0.032**
Monocytes/µl	A	321.9 (228-503)	376.8 (210.6-658.5)	398 (274.8-732.8)	0.872	0.833	0.640	0.766
	D	397 (347-595)	636 (472-1057)		0.099	0.055	0.890	0.112
Basophils/µl	A	15.09 (6.35-31.77)	31.2 (16.9-42.32)	31.6 (16.4-63)	0.150	0.550	0.077	0.152
	D	19.56 (10.1-26.8)	30.9 (15.86-54.2)		0.273	0.589	0.109	0.364
Eosinophils/µl	A	12.5 (5.5-40.88)	24.39 (6.85-60.18)	114.8 (96.48-297)	**<0.001**	**<0.001**	**<0.001**	0.602
	D	116 (36.95-142.7)	42 (23.21-58.41)		**0.008**	**<0.001**	0.364	0.190
DETECTABLE SARS-CoV-2 PLASMA Viral Load, n (%) [c]	A	3 (33%)	10 (91%)	NA	**0.007**	NA	NA	**0.007**
	D	0 (0%)	0 (0%)					
SARS-CoV-2 PLASMA Viral Load in patients with detectable levels (cps/ml)	A	111.7 (33.91-563.5)	131 (36.1-713)	NA	NA	NA	NA	0.864
	D	NA	NA	NA	NA	NA	NA	NA
Treatment [c]: Dexametasone, n (%) Other glucocorticoids, n (%) Tocilizumab,n (%) Lopinavir/Ritonavir, n (%) Remdesivir, n (%)		 1 (11) 1 (11) 0 (0) 6 (68) 2 (22)	 4 (36) 5 (45) 3 (27) 2 (18) 4 (36)	NA	 0.293 0.619 0.507 0.123 0.632	NA	NA	 0.293 0.619 0.507 0.123 0.632

Values expressed as medians (interquartile range) unless otherwise specified. P/f: Ratio of the partial pressure of arterial oxygen to the fraction of inspired oxygen; CRP: C reactive protein; PCT: procalcitonin; Ferritin: A: Admission; D: Discharge. NA: Not Applicable. Comparisons were done using [a]) One way ANOVA unless otherwise stated; [b]) Mann–Whitney U-test unless otherwise stated; [c]) Chi-squared test.

As expected, ICU patients featured longer hospital stay and had a significant reduction in their ratio of the partial pressure of arterial oxygen to the fraction of inspired oxygen (P/f)

when compared to the No-ICU in both admission and discharge. ICU patients also showed increased C-reactive protein (CRP) at admission, which has been described a marker for COVID-19 severity (Ali, 2020). Interestingly, no difference was found between the levels of procalcitonin (PCT), Ferritin, D-dimers and Lactate Dehydrogenase (LDH). Nearly all ICU patients (91%) had detectable SARS-CoV-2 plasma viral load at admission, but not at discharge, contrasting to only 33% of the No-ICU patients at admission. Circulating leukocytes counts were altered in the ICU group at admission, having a significant reduction of lymphocytes and a simultaneous increase of neutrophils that lead to a reduced lymphocyte/neutrophil ratio. Eosinophils were also greatly reduced at both admission and discharge from the ICU. Of note, the counts of monocytes remained unaltered in both groups.

To analyse circulating monocytes and DCs, the circulating leukocytes from whole blood samples were stained using the panel described in **Table 1**. Then, the main populations were defined utilizing the gating strategy illustrated in **Figure 3**. After debris and doublet exclusion, monocytes and DCs were defined within cells expressing the CD45 and negative for the lineage markers CD3, CD19 and CD66b ($CD45^{+}Lin^{-}$). Monocytes subsets were defined by their expression of CD14 and CD16 according to the gating strategy described by Zawada et al (Zawada *et al.*, 2015): Classical monocytes ($CD14^{high}CD16^{-}$); Intermediate monocytes ($CD14^{high}CD16^{+}$); Non-Classical ($CD14^{low/-}CD16^{+}$). The two mDCs subsets were defined within the CD45+Lin- gate by positive expression of HLA-DR and either CD141, defining the $CD141^{+}$ mDCs or CD1c, defining the $CD1c^{+}$ mDCs. pDCs were defined by their positive expression of CD123 and HLA-DR. Basophils were defined as positive for CD123 but negative for HLA-DR.

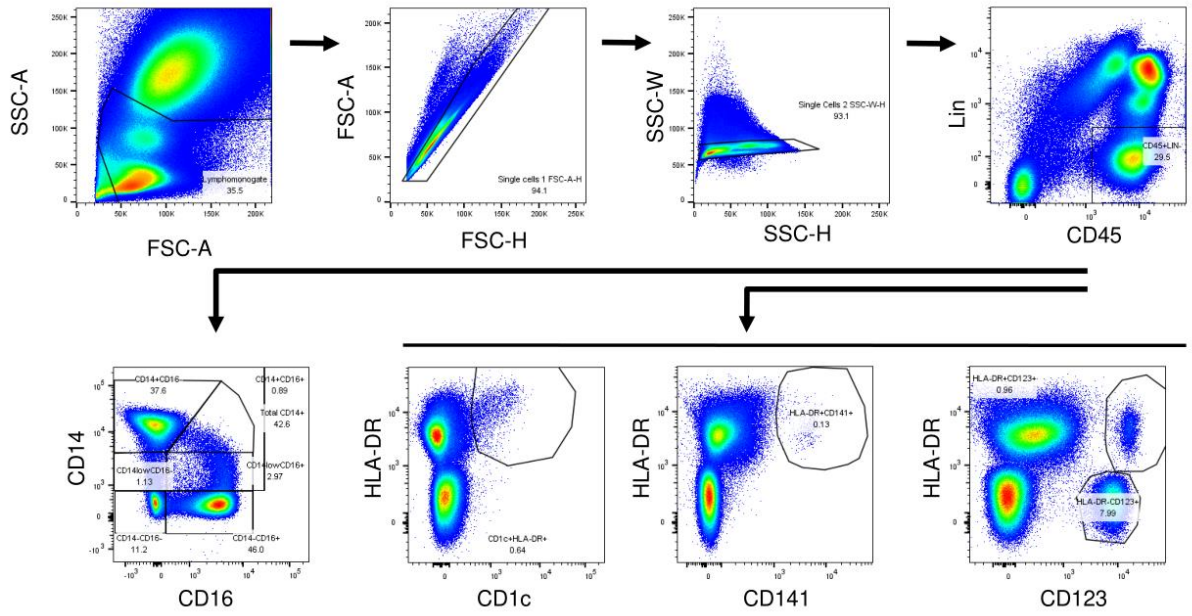

Figure 3 –**Gating strategy used to identify monocytes and dendritic cells from whole blood of COVID-19 patients**
Dot plots showing data from a representative healthy control, starting from 10 M leukocytes stained.

To perform the unsupervised analysis, a $CD45^{+}Lin^{-}$ dataset was created by taking the same number of $CD45^{+}Lin^{-}$ cells from all samples. UMAP was applied to the dataset and then clustered using the X-Shift algorithm, obtaining 16 clusters (**Figure S1**). The clusters were then annotated into 10 subsets based on the marker expression, defining the major circulating monocyte and DC populations (**Figure 4A-B**). These subsets included the several subpopulations of classical monocytes and non-classical monocytes. Within the classical monocytes ($CD14^{high}CD16^{-}$) were identified two subsets that showed a M2-like phenotype. The first one had the highest levels of CD163, low/intermediate HLA-DR, CD86 and low CD80 and was designated as $CD163^{++}$ M2-like. The other subset shared the same M2 profile but had high HLA-DR and positive PD-L1 and was named as PD-$L1^{+}$ M2-like. It was also possible to identify two non-classical monocyte subsets ($CD14^{low/-}CD16^{+}$) based on their Slan expression. The main subsets of DCs were also identified, the CD1c+ mDCs (HLA-DR^{high} $CD1c^{+}$), the CD141+ mDCs (HLA-DR^{high} $CD141^{+}$) and pDCs (HLA-$DR^{high}CD123^{+}$) (**Figure 4B**). To assess phenotypic changes during disease course, the relative frequencies of all subsets in each timepoint and group were evaluated (**Figure 4C**). Both the No-ICU and ICU showed noticeable changes in subset frequencies at admission and discharge. Some of the DC and non-classical monocyte subsets appeared decreased in both groups, while the M2-like subsets were expanded in COVID-19 patients.

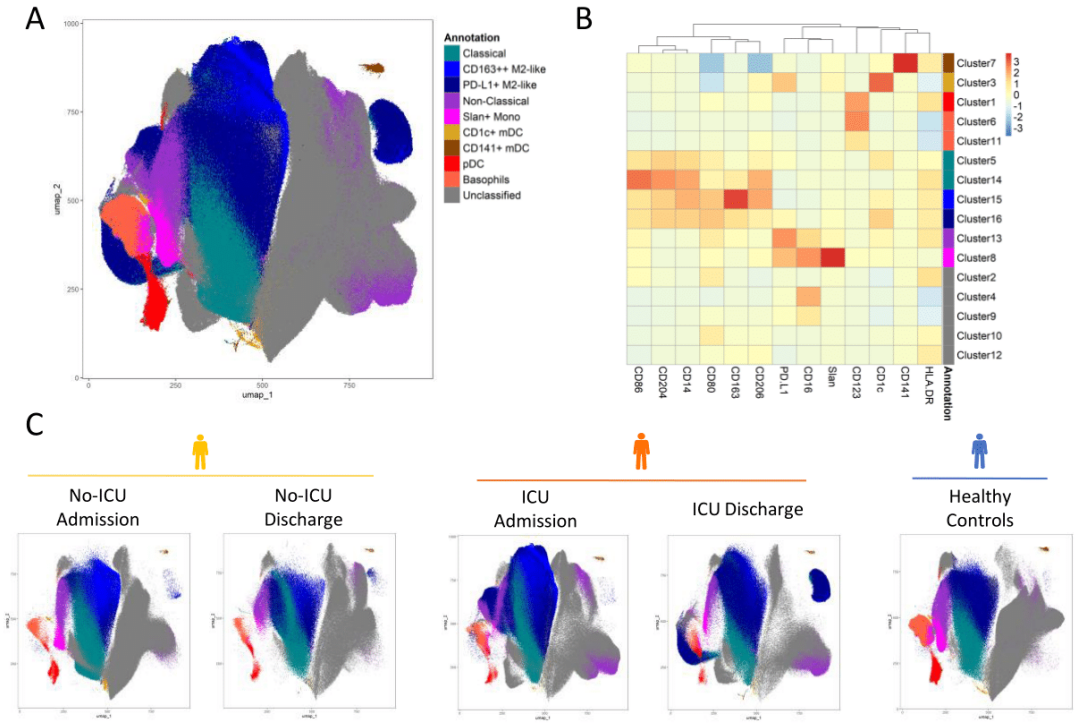

Figure 4 – **Phenotyping circulating monocytes and dendritic cells in severe COVID-19 recovery.**
(A) UMAP of the $CD45^{+}Lin^{-}$ dataset displaying the main subsets annotated. (B) Heatmap showing the relative marker expression of the clusters obtained with X-shift and their respective annotation. (C) Relative subset distribution in patients at admission/discharge and in healthy controls. Healthy controls (blue), No-ICU patients (yellow) and ICU patients (orange).

3.1.2. Assessing phenotypic changes in monocytes from patients with severe COVID-19

Further analysis of the monocyte subsets frequencies revealed the depletion of non-classical monocytes expressing Slan (Slan^{+} Mono) compared to healthy controls, in both No-ICU and ICU patients, persisting at discharge, being more evident on the ICU group (

Figure 5**A**). The Slan negative non-classical monocyte subset did not show any significant changes.

Interestingly, both M2-like classical monocyte subsets were expanded, but only significantly in the ICU group (

Figure 5**B-C**). The CD163^{++} M2-like highest frequencies were at ICU admission and was still significantly expanded at discharge, despite a decline in frequency (

Figure 5**B**). Interestingly, the only subset that increased between admission and discharge was the PD-L1^{+} M2-like subset, already expanded at ICU admission but with the highest percentages at discharge (

Figure 5**C**). No significant changes in the frequency of the less differentiated classical monocyte subset were found.

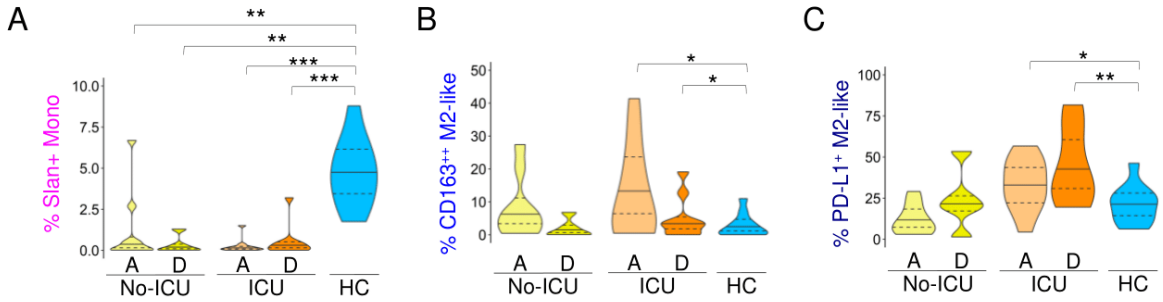

Figure 5 –**Slan^{+} non-classical monocytes were depleted in severe COVID-19 while the M2-like subsets expanded.**
Violin graphs showing annotated monocyte subsets frequency within CD45^{+}Lin^{-} cells: **(A)** Slan^{+} Mono; **(B)** CD163^{++} M2-like; **(C)** PD-L1^{+} M2-like. Comparisons were performed between patient groups and healthy controls using Mann–Whitney U-test. p values are shown as ***p < 0,001; **p < 0,01; *p < 0,05. No statistical differences were found between patient groups. ICU, Intensive care unit; A, admission; D, Discharge; HCs, Healthy controls.

To confirm the observations made with unsupervised analysis, monocyte populations were evaluated using the previously described gating strategy (**Figure 6**). Although total monocytes count remained unchanged in all COVID-19 patients (**Table 3**), there were significant changes to the counts of classical and non-classical populations compared to HCs. Non-classical monocyte counts were globally depleted in both groups at both timepoints. In contrast, classical monocyte counts were expanded at discharge in ICU patients (**Figure 6A**).

There was an increased M2-like profile in classical monocytes (CD14^{high}CD16^{-}) at discharge of ICU patients. This profile was characterized by the increased expression of CD163 at discharge, the increase in cells expressing both CD204 and CD206 and the simultaneous decrease in cells expressing CD80 and CD86. Further confirming the

unsupervised analysis, a significant increase in classical monocytes expressing PD-L1 in ICU patients at discharge was observed (**Figure 6B**).

Regarding the profile of non-classical monocytes ($CD14^{low/-}CD16^{+}$), the significant contraction of the Slan positive population was confirmed. Interestingly, an increase was observed in non-classical monocytes lacking CD80 and CD86 expression, showing that non-classical monocytes profile was also affected by severe COVID-19 together with their significant depletion.

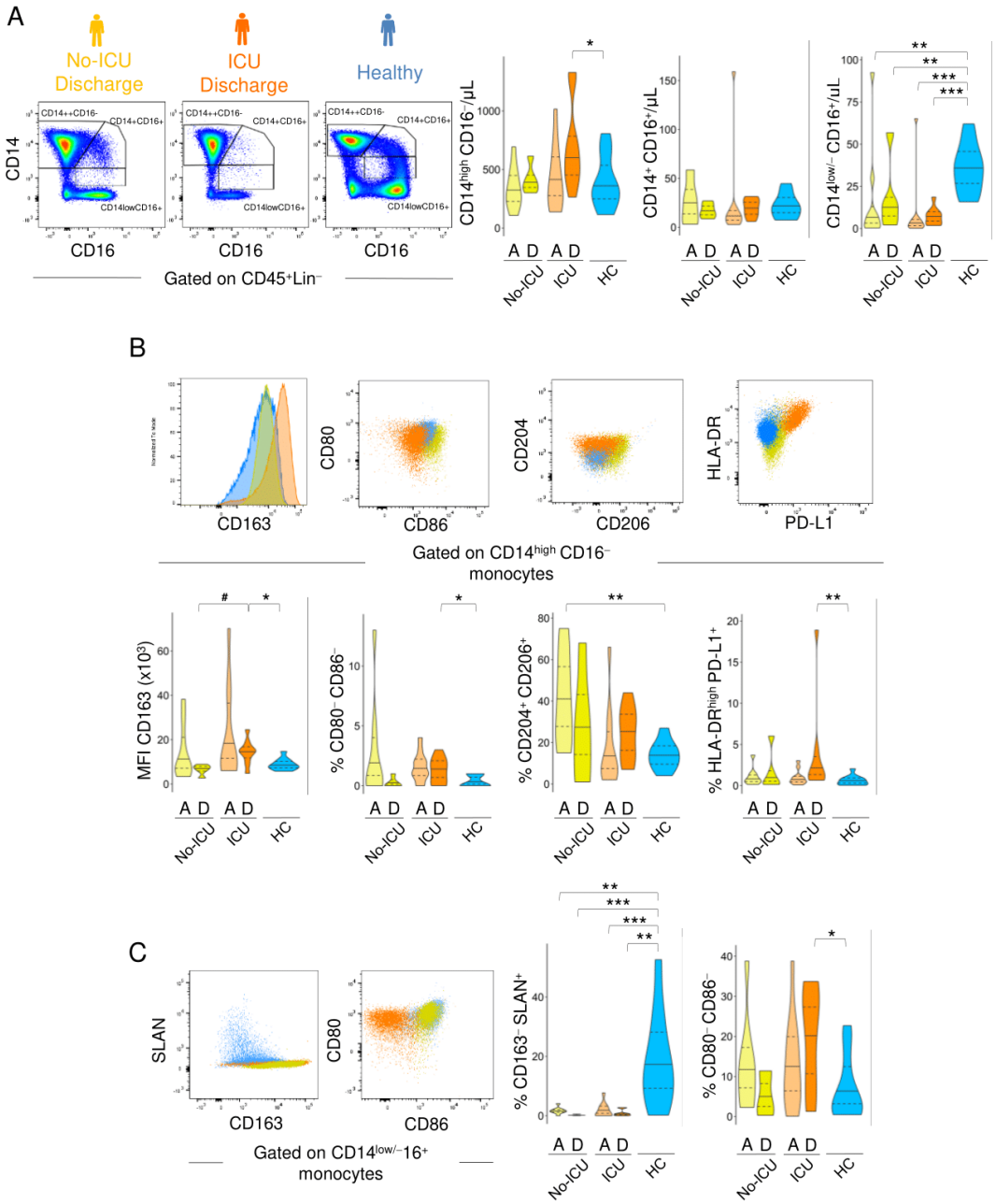

Figure 6 – **Rise of the immunomodulatory phenotype in classical monocytes was confirmed by gating analysis.**
(A–C) Illustrative dot plots of a representative No-ICU patient (yellow) and in an ICU patient at discharge (orange), as well as in a healthy control (blue); **(A)** Violin graphs showing absolute counts of the main monocyte subsets; **(B)** CD163 MFI and proportion of $CD80^{-}CD86^{-}$, $CD204^{+}CD206^{+}$, and $HLA\text{-}DR^{high}PD\text{-}L1^{+}$ subsets within classical ($CD14^{high}CD16^{-}$) monocytes; **(C)** Proportion of $CD163^{-}Slan^{+}$ and $CD80^{-}CD86^{-}$ within non-classical ($CD14^{low/-}CD16^{+}$) monocytes. There were no significant differences between admission and discharge in both ICU

and No-ICU patient groups (Wilcoxon matched-pairs signed rank test). Other comparisons were done using Mann–Whitney U-test and significant P values are shown: ***p < 0,001; **p < 0,01; *p < 0,05, as compared to healthy; #p < 0,05, as compared to No-ICU at the same time-point.

Given the potential impact of the increased immunomodulatory phenotype in disease course, possible associations between the length of hospital stay and the humoral response were evaluated (**Figure 7**). As was expected from the previous results, only the PD-L1^{+} M2–like subset had a significantly positive correlation with both hospital stay and time since symptoms onset (**Figure 7A**). Interestingly, the expansion of this immunomodulatory population also correlated with the increase of antibody titres (**Figure 7B**), indicating that possibly common mechanisms contribute to the humoral response and the rise of the M2-like phenotype. It was also evaluated if the rise of this phenotype was associated with active viral replication (**Figure 7C**). The PD-L1^{+} M2-like subset was the only subset that was significantly enriched in viremic patients.

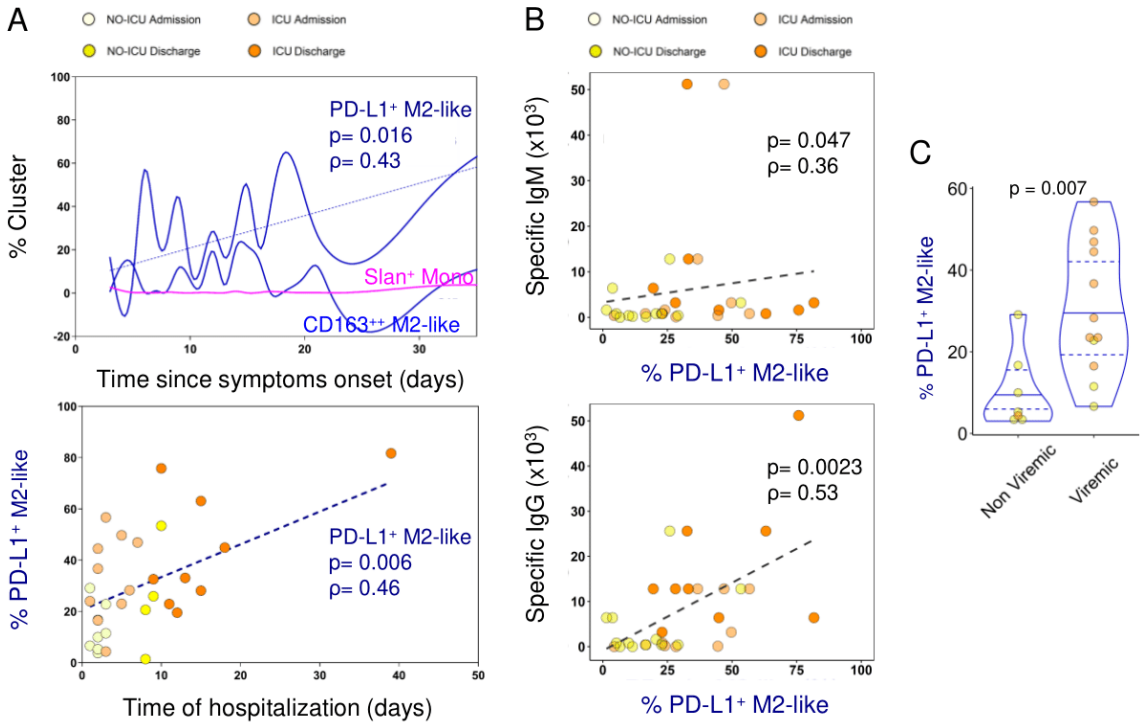

Figure 7 – **M2-like phenotype expanded until discharge, especially in patients with viremia and correlated with mounting antibody response**.
(A) Correlation of indicated subset frequencies with days since symptoms onset (top) and time of hospitalization (bottom). **(B)** Correlation between PD-L1+M2-like frequency and anti-SARS-CoV-2 specific IgM (top) and IgG (bottom) titers; Spearman Rank correlation coefficient was used. **(C)** Frequency of PD-L1+M2-like at admission in viremic versus non-viremic patients; comparison done using Mann-Whitney U-test. Significant p-values shown (p<0.05).

3.1.3. Circulating dendritic cell phenotype in severe COVID-19 recovery

The relative frequencies identified DCs subsets were evaluated (**Figure 8**). pDCs were significantly depleted in all timepoints of both ICU and No-ICU patients when compared to healthy controls (**Figure 8A**). Conversely, the CD141^{+} mDC subset was also reduced in all time points and groups but showed a slight recovery at discharge in No-ICU patients (**Figure**

8B). No significant changes were found for the CD1c$^+$ mDC subset, however there was a trend towards decrease in ICU patients from admission (ICU A: 0.05, 0.03-0.12; HC: 0.13, 0.08-0.34; p = 0.058) to discharge (ICU D: 0.04, 0.03-0.13; HC: 0.13, 0.08-0.34; p = 0.056) (**Figure 8C**).

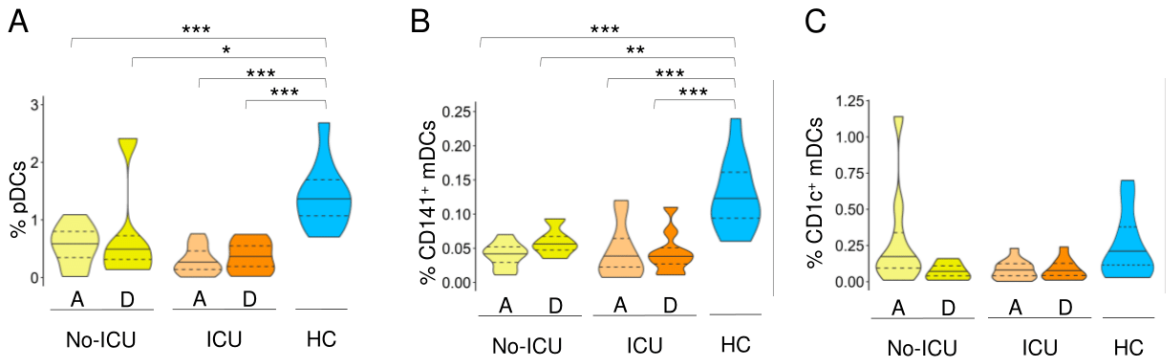

Figure 8 – **pDCs and CD141+ mDC are depleted in COVID-19.**
Violin graphs showing annotated dendritic cell subsets frequency within CD45$^+$Lin$^-$ cells: **(A)** pDCs; **(B)** CD141$^+$ mDCs; **(C)** CD1c$^+$ mDCs. Comparisons were performed between patient groups and healthy controls using Mann–Whitney U-test. p values are shown as ***p < 0,001; **p < 0,01; *p < 0,05. No statistical differences were found between patient groups. ICU, Intensive care unit; A, admission; D, Discharge; HCs, Healthy controls.

An analysis with manual gating directed at DCs was made to assess phenotypic changes (**Figure 9**), revealing that all DC populations were altered in COVID-19. pDCs showed the most striking depletion, being reduced in both groups, at all timepoints (**Figure 9A**).

Both myeloid dendritic cells (mDCs) were reduced, but at different timepoints, with CD141$^+$ mDCs reduced at discharge in both groups (**Figure 9B)** and CD1c$^+$ mDCs reduced at admission of both groups (**Figure 9C**).

The profile observed in the DC population was reminiscent of the immunomodulatory profile observed in circulating monocytes. Namely, an increased expression of the scavenger receptors CD204, CD163 and CD206 in both pDCs and CD141$^+$ mDCs was observed, persisting until discharge, only in ICU patients. The more severe ICU patients also featured an increased expression of PD-L1 in pDCs and CD141$^+$ mDCs at discharge (**Figure 9 D-E**), mirroring the phenotype seen in classical monocytes. The only change in the phenotype of CD1c$^+$ mDCs was a decreased expression of CD204 and CD206 at the admission of No-ICU patients (**Figure 9F**).

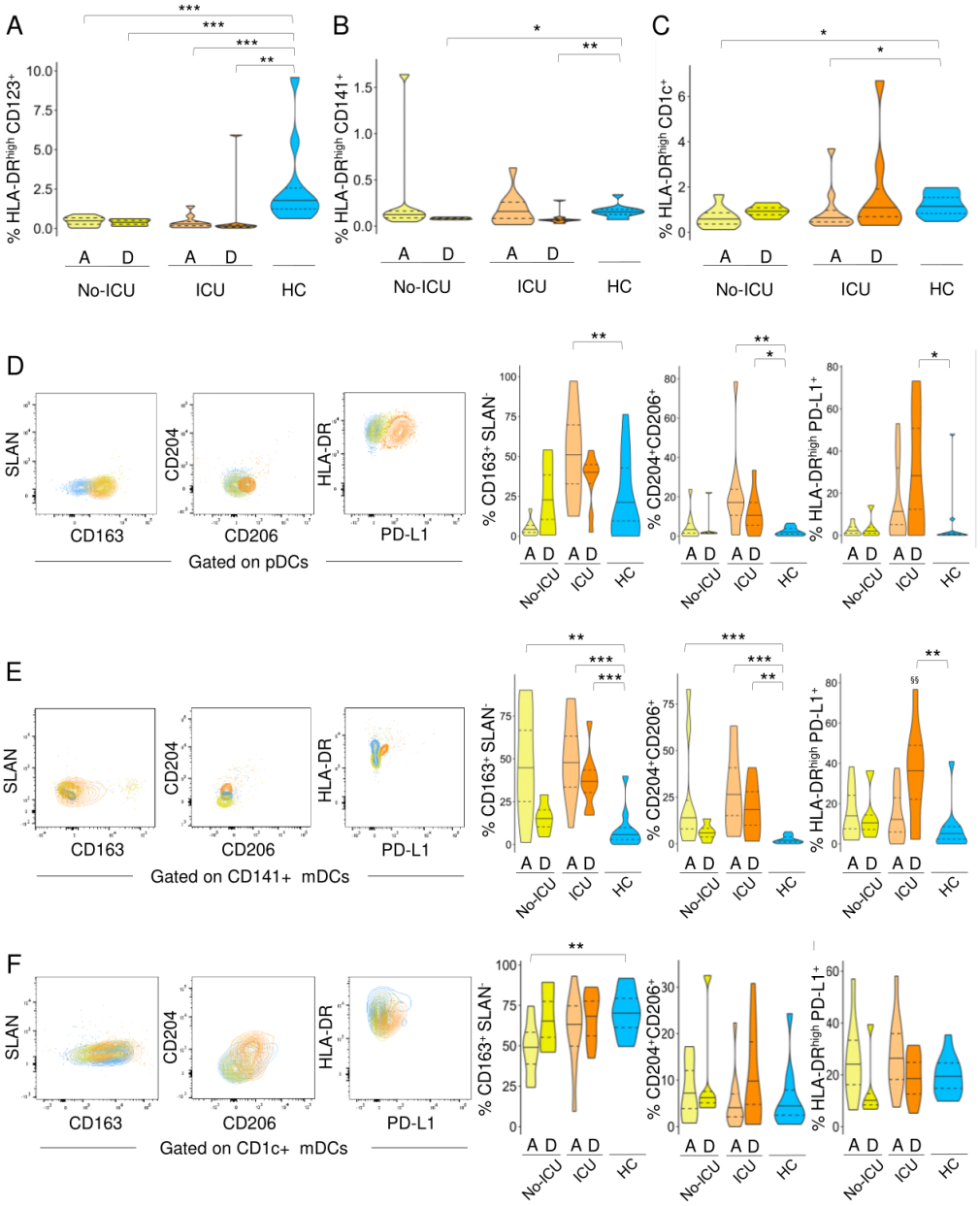

Figure 9- **DC populations also show an immune regulatory phenotype.**
Frequency of HLA-DR^{high}CD123^{+} (pDC) population **(A)**, HLA-DR^{high} CD141^{+} (CD141^{+}mDC) population **(B)** and HLA-DR^{high} CD1c^{+} (CD1c^{+}mDC) population **(C)** within total CD45+Lin− cells. **(D–E)** Illustrative dot-plots (left) of bi-dimensional hierarchical gating strategy were used to analyse the phenotype of pDCs **(D)**, CD141^{+}mDCs **(E)** and CD1c^{+}mDCs **(F)**from No-ICU (yellow) and ICU (orange) patients at discharge and healthy control (blue) and the respective graphs (right). Wilcoxon matched-pairs signed rank test of the paired analysis of the two-time points and significant P values are shown: §§p < 0,01. Mann–Whitney U-test were used for comparison with healthy controls: ***p < 0,001; **p < 0,01; *p < 0,05.

3.1.4. Correlation of the specific phenotypic changes with serum cytokine levels at different stages of severe COVID-19

We aimed at investigating if the immunomodulatory phenotype seen in circulating monocyte and dendritic cell populations could be accompanied with a specific cytokine environment that promoted this profile.

So, the possible relations between monocytes subsets and DC populations identified with circulating serum levels of 71 cytokines and chemokines were investigated (**Figure 10**).

The expansion of the PD-L1^{+} M2-like and the CD163^{++} M2-like subsets had a negative correlation with the levels of several pro-inflammatory cytokines and chemokines related to the IFN response, such as IP-10, CXCL9 and IL12-p40 (**Figure 10A**). On the other hand, the decline of the non-classical monocyte subsets had positive correlation with the levels of Macrophage inflammatory protein-1 beta (MIP-1β/CCL4), IL-21, CXCL9 and IL-1α. Similarly, the expansion of pDCs and CD141+ mDCs immunomodulatory phenotype also had an inverse correlation with analytes related to the IFN response, TNF-α pathway and acute phase response (**Figure 10B**). No correlations were found with CD1c^{+} mDCs. In summary, the results indicated that the rise of the immunomodulatory profile in severe COVID-19 recovery was accompanied by a decrease in pro-inflammatory signals, making immune regulation the predominant state at recovery.

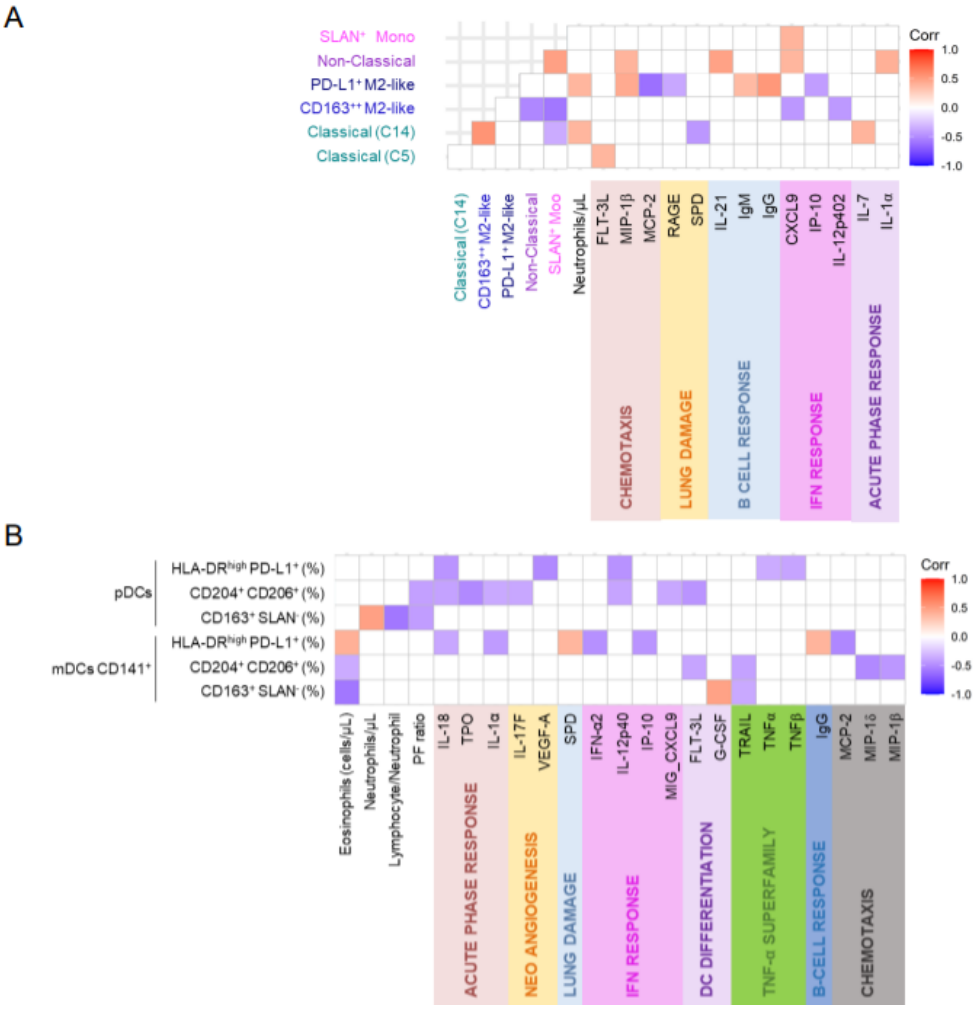

Figure 10 – **The immunomodulatory phenotype in circulating monocytes and DCs correlated with the decline of pro-inflammatory cytokines and chemokines.**
Correlation matrix identifying relations between the frequency of the annotated monocyte clusters **(A)** and the populations within pDCs and CD141+mDCs **(B)** with serum markers from both time-points and from patient and control groups; Spearman Rank correlation coefficient was used and significant correlations (p-values < 0.05) are shown.

To better describe the immunomodulatory state and cytokine environment during severe COVID-19 recovery, 42 of the 71 analytes measured that showed significant changes between

patients and HCs or within the patients groups or demonstrated by previous studies to be associated with the cytokine storm in severe COVID-19 (Haljasmägi *et al.*, 2020) were selected. To define the analytes that better segregated the patients from HCs and admission from discharge, a principal component analysis was performed (**Figure 11A**).

The analytes with the highest loading scores in the principal components and the relevant monocytes and DCs subsets described above were clustered using hierarchical clustering (**Figure 11B**). The COVID-19 patients were characterized by the depletion of the $Slan^{+}$ non-classical monocytes, $CD141^{+}$ mDCs and pDCs.

The admission stage of ICU and No-ICU patients showed the highest levels of several pro-inflammatory cytokines and the increased frequencies of the $CD163^{++}$ M2-like classical monocyte subset.

Confirming the previous observations, the PD-$L1^{+}$ M2-like subset was the only subset that characterized the discharge of ICU patients. Notably, ICU patients at discharge maintained significantly elevated levels of the pro-inflammatory cytokine IL-6, but also of the immunomodulatory cytokines IL-1RA and IL-10 in parallel with the expanded PD-L1+ M2-like subset (**Figure 11C,** highlighted section).

Taking everything into consideration, these results show that the recovery from severe COVID-19 was associated with a shift in the phenotype of circulating monocytes and dendritic cells towards an immunomodulatory or M2-like phenotype. The shift was associated with the decrease of plasma viral load and pro-inflammatory cytokines, while elevated immune regulatory cytokines were maintained and the humoral response mounted.

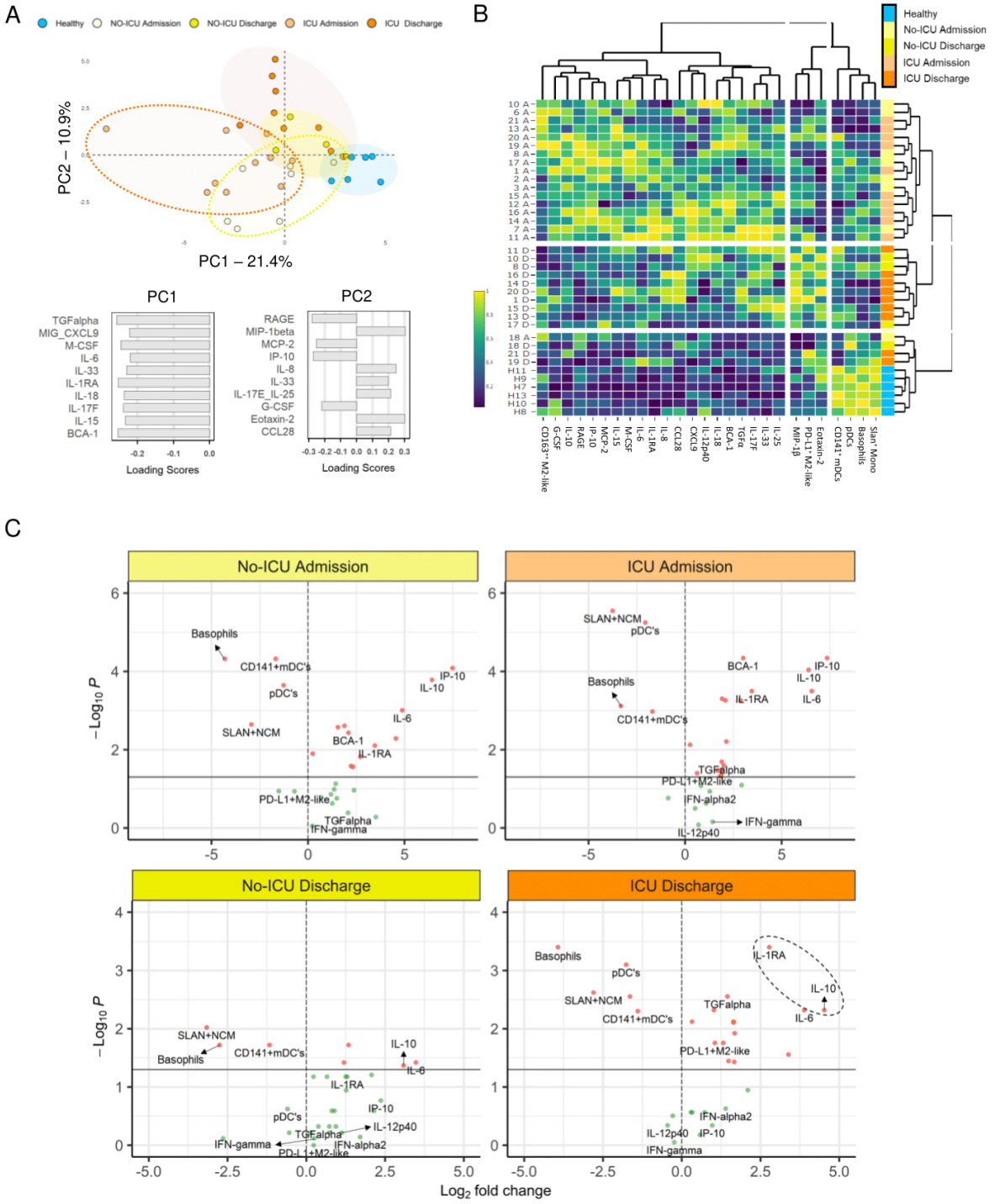

Figure 11 – **Monocyte and DC subsets and immunoregulatory serum markers segregate COVID-19 stages**. **(A)** Principal component analysis (PCA) of the 35 analytes showed significant different serum levels in healthy subjects or in patients between the time-points analysed. Loading scores of principal component 1 (PC1) and PC2 showing the top 10 highest absolute values. **(B)** Heatmap performed using the top 10 parameters in the PC1 and PC2 of the PCA analysis showed in **(A)** and the frequencies of the annotated subsets found to be significantly altered in COVID-19 patients; dendrograms illustrate the hierarchical clustering. **(C)** Volcano plots comparing the variables used in the heatmap showed in **(B)** patient groups and healthy controls; a p value < 0.05 was considered significant.

3.2. Monocyte Profile in a Case Study of an Acute HIV-1 Infected Patient in Comparison with Acute SARS-CoV-2 Infection

3.2.1. Characterization of the circulating monocytes and dendritic cells in acute HIV−1 compared to SARS-CoV-2 infection using unsupervised analysis

In parallel with the COVID-19 patient cohort, we were able to study an early acute HIV-1 infected individual. The acute HIV-1 infected patient was classified as in Fiebig stage two, showing high plasma viral load and detectable p24 antigenemia and no serum HIV antibodies (Fiebig *et al.*, 2003). The patient presented to clinical attention with fever and asthenia continuing from 13 days and elevated aminotransferases, showing signs compatible with HIV−induced hepatitis and acute inflammatory response. The patient's circulating monocyte and DC profile was compared to 20 acute SARS-CoV-2 infected individuals from the previous study, one ART naïve chronic HIV-1 infected individual and eleven healthy controls (**Table 4**).

Table 4 - **Clinical Data and Blood Work from acute HIV-1 and COVID-19 patients and Healthy Controls**

	HIV-1 Acute	HIV-1 Chronic	COVID-19*	Healthy Controls
Number (males)	1 (0)	1 (1)	20 (17)	11 (9)
Age (years)	22	49	55.5 (39-65)	58 (39-65)
Time from symptoms start (days)	13	NA	8.5 (5-11)	NA
CRP (mg/dl)	2.60	0.37	8.8 (4.85-25.5)	ND
PCT (ng/ml)	0.48	ULoD	0.16 (0.11-0.38)	ND
Ferritin (ng/ml)	412	262	939 (402-1 906)	ND
Interleukin 6 (pg/ml)	1.5	2.8	18 (4.5-36)	0.85 (0.24-1.6)
Lymphocytes/ml	1 620	3 130	920 (845-1 662)	1 940 (1 423-2 200)
CD4+ T /ml	364	210	247 (133-392)	768 (544-998)
CD8+ T /ml	503	863	145 (81.2-262)	414 (158- 577)
CD4/CD8 ratio	0.72	0.24	1.78 (0.93-2.50)	1.95 (1.53-4.17)
Neutrophils/ml	1 830	2 290	4 251 (2 413-6 917)	3 228 (2 521-6 390)
Lymphocytes/neutrophils ratio	0.89	1.37	0.23 (0.15-0.5)	0.51 (0.47-0.61)
Monocytes/ml	810	720	349 (223-537)	398 (275-733)
Basophils/ml	10	50	20 (9.7-35)	32 (16-63)
Eosinophils/ml	30	200	13 (6.7-56)	115 (96-297)
SARS-CoV-2 Plasma Viral Load[#] (RNA cps/ml)	NA	NA	112 (24-498)	NA
HIV-1 Plasma Viral Load (RNA cps/ml)	1 320 000	57 200	NA	NA

Values expressed as medians (interquartile range) unless otherwise specified. CRP: C reactive protein; PCT: procalcitonin; NA: Not Applicable; ND: Not Done; ULoD: Under Limits of dectection.*COVID-19 associated co-morbidities: Arterial hypertension 9 (45%); Diabetes type II 6 (30%); Obesity 6 (30%); Lung emphysema 2 (10%); no co-morbidities in HIV-1 infected patients; [#]Qauntified in the 13 out of 20 COVID-19 patients with detectable SARS-CoV-2 plasma viral load.

As expected, in the acute phase of HIV-1 and SARS-CoV-2 infection, patients showed signs of an ongoing inflammatory response, with elevated levels of CRP and ferritin, although this profile was more pronounced in COVID-19 patients. COVID-19 patients also showed elevated levels of IL-6, which has been described as a mainstay of the cytokine storm of SARS-CoV-2 infection.

Circulating leukocyte counts were altered in all patients, with COVID-19 patients featuring an accentuated neutrophilia and lymphopenia. Despite the acute HIV-1 patient showing normal lymphocyte levels, the CD4/CD8 ratio was altered due to a decrease in $CD4^+$

T-cells. The chronic HIV-1 patient showed the most striking changes in the lymphocyte compartment with an accentuated decrease in $CD4^+$ T-cell accompanied by an expansion of $CD8^+$ counts, leading to the lowest CD4/CD8 ratio. Interestingly, the monocyte counts of both HIV-1 infected individuals was higher compared to COVID-19 patients and healthy controls.

To explore the profile of circulating monocytes and DCs, whole blood samples were stained using the antibody panel showed in (**Table 1**). The main monocyte and dendritic populations were defined using the new gating strategy illustrated in **Figure 12**. Similar to the previous gating strategy, after doublets and debris removal, monocyte and DC populations were studied within the cells expressing CD45 but not the lineage markers CD3, CD19 and CD66b ($CD45^+Lin^-$). Then the populations of DCs were sequentially defined and separated, starting with the pDCs ($HLA\text{-}DR^{high}CD123^+$). Basophils percentages were also evaluated ($HLA\text{-}DR^-CD123^+$). Then, inside the $CD123^{-/low}$ cells the $CD141^+$ mDCs ($HLA\text{-}DR^{high}CD141^+$) were defined. The final population of DC defined was the $CD1c^+$ mDCs ($HLA\text{-}DR^{high}CD1c^+$) within the $CD141^{-/low}$ cells. The monocytes were then defined within the $CD1c^{-/low}$ cells as CD86 and HLA-DR positive to remove non-monocytes cells. Finally, the three monocyte subsets were defined based on CD14 and CD16 expression: Classical ($CD14^{high}CD16^-$), Intermediate ($CD14^{high}CD16^+$), Non-Classical ($CD14^{low/-}CD16^+$) monocytes.

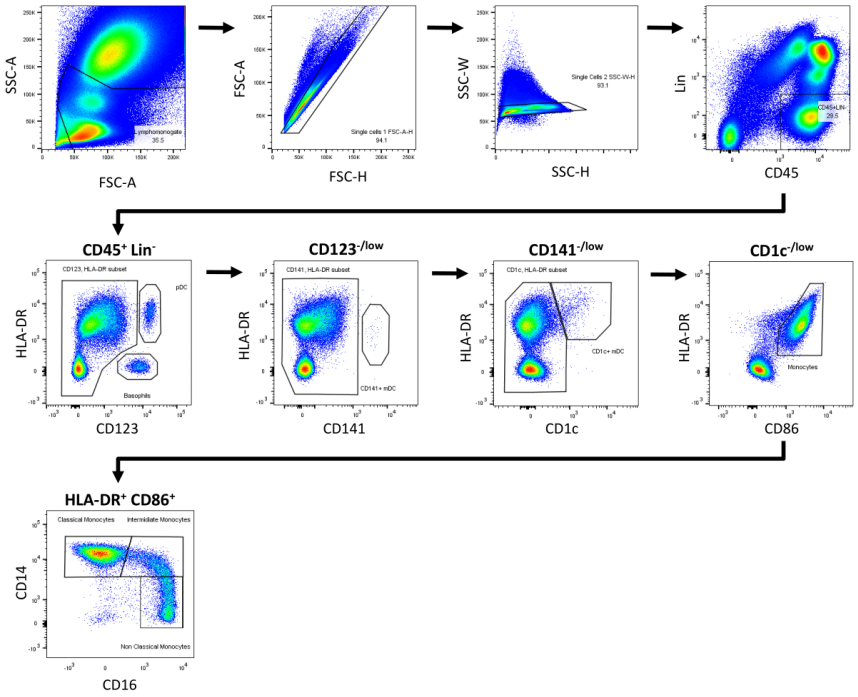

Figure 12 – **Gating strategy for profiling monocyte and in acute HIV-1 and SARS-CoV-2 patients**.
Illustrative gating strategy used to identify monocyte and dendritic cells from whole blood, starting from 10 million leukocytes. Dot plots showing data from a representative healthy control.

To explore the phenotype in acute infection, an unsupervised analysis was performed on the $CD45^+Lin^-$ dataset, using UMAP and clustering with FlowSOM, obtaining 14 clusters **(Figure S2)**. The clusters were then annotated into 10 subsets based on marker expression

(Figure 13A), identifying the main subsets of monocytes and dendritic cells. Within classical monocytes, it was possible to distinguish two subsets that showed opposite polarizations. The first one displayed a M1-like phenotype with low CD163 expression and positive CD80 and CD86 expression. The second subset showed a M2-like polarization with high CD163 expression, positive CD204 and CD206 while maintaining lower levels of CD80 and CD86. It was possible to distinguish two non-classical monocyte subsets based on the Slan expression.

Notably, when analysing the distribution of the subsets, the acute HIV-1 and COVID-19 patients shared the depletion of the Slan^{+} non-classical monocyte subset (Slan^{+} Mono), which was showed normal levels in the HCs and in the chronic HIV-1 patient. It was also evident that the distribution of the M1-like and M2-like monocyte subsets differed among the two acute infections **(Figure 13B)**.

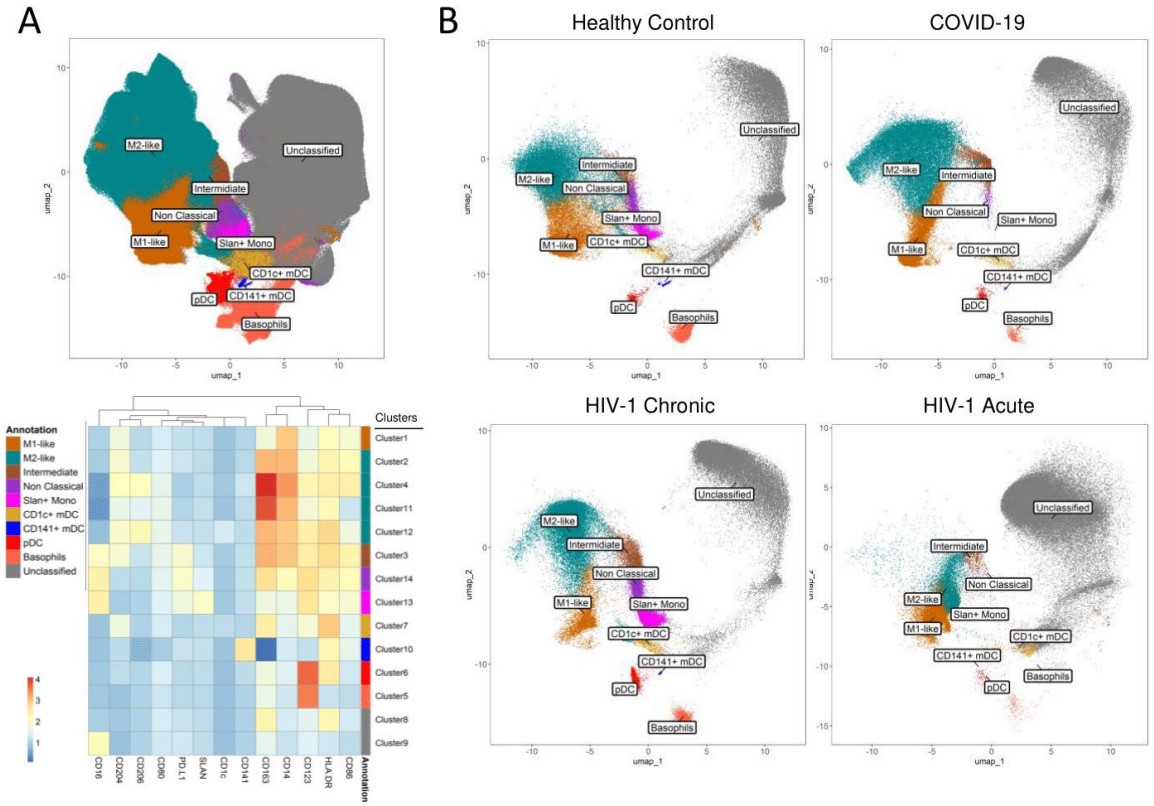

Figure 13 - **Profiling monocytes and DCs in HIV-1 and SARS-CoV-2 infections using unsupervised analysis**.
(**A**) UMAP of the CD45^{+}Lin^{-} dataset of all samples with the heatmap showing relative marker expression of the clusters obtained with the FlowSOM clustering algorithm and the manual annotation of the main subsets. **(B)** Relative subset distribution in representative individuals from the healthy control and COVID-19 groups, as well as in the untreated HIV-1 acute and HIV-1 chronic patients.

3.2.2. Exploring monocyte phenotype and subpopulations distribution in acute HIV-1 infection

The evaluation of monocyte subset frequencies showed that the acute HIV−1 infected patient had a two-fold increase in the frequency of the M1-like classical monocyte subset when compared to HCs, while the SARS-CoV-2 infected patients showed decreased frequencies of

the same subset. The M2-like subset was substantially reduced in the acute HIV-1 patient when compared to the COVID-19 patients and healthy controls (**Figure 14A**).

The other striking feature observed was the decrease of the non-classical monocyte subsets in both acute HIV-1 and SARS-CoV-2 infection, especially the Slan^{+} subset which was depleted in most of the acute patients (**Figure 14B**). Using manual gating, it was possible to confirm the reduction of non-classical monocytes in both acute infections (**Figure 14C**) and the depletion of the Slan^{+} population (**Figure 14D**).

Interestingly, the chronic HIV-1 patient maintained a high frequency of the M1–like phenotype in circulating monocytes, reminiscent of the profile observed in the acute HIV-1 patient. However, the Slan^{+} non-classical monocytes appeared instead expanded in this patient, which is in accordance with previous studies on chronic viremic HIV-1 patients (Dutertre *et al.*, 2012; Tufa *et al.*, 2016).

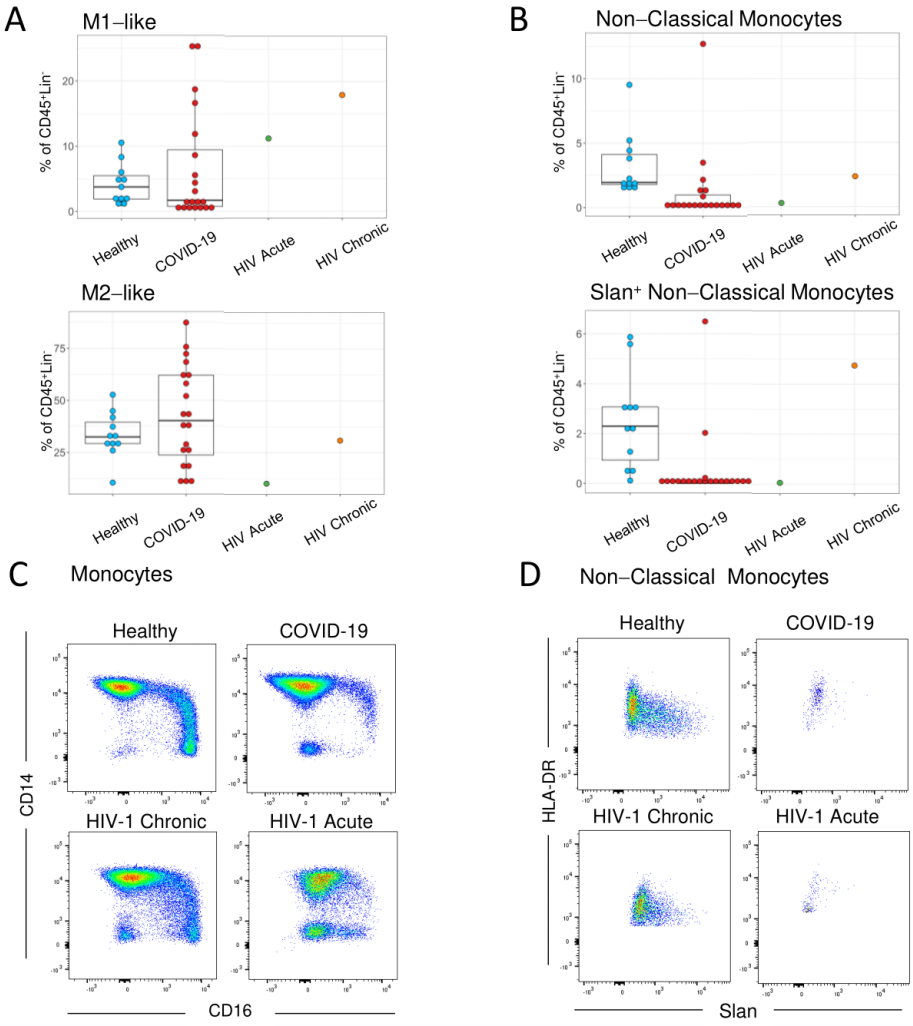

Figure 14 – **Shift to M1-like profile and loss of Slan+ Monocytes in acute HIV-1 infection.** (**A**,**B**) Boxplots showing the frequencies medians and interquartile range of the identified subsets using FlowSOM, as shown in **Figure 13**. Each dot represents one subject. (**C**,**D**) Illustrative dot plots of the manual analysis performed in representative individuals from the healthy control and COVID-19 groups, as well as in the HIV-1 acute and untreated HIV-1 chronic patients showing the expression of CD14 and CD16 in monocytes (**C**); and the expression of HLA-DR and Slan in the non-classical (CD14$^{low/-}$CD16^{+}) monocytes (**D**).

3.2.3. Dendritic cell phenotype in acute HIV-1 infection

Regarding the profile of the mDCs, the CD141$^+$ mDC subset was also reduced in both the acute HIV-1 and SARS-CoV-2 patients, the CD1c$^+$ mDC subset was relatively unchanged (**Figure 13A**). However, the profile of the CD1c$^+$ mDC was altered, showing higher expression of the activation markers CD80 and CD86 (**Figure 13B**). On the other hand, pDCs also showed decreased frequencies in the acute infections (**Figure 13A**), but no noticeable changes in phenotype (**Figure 13B**).

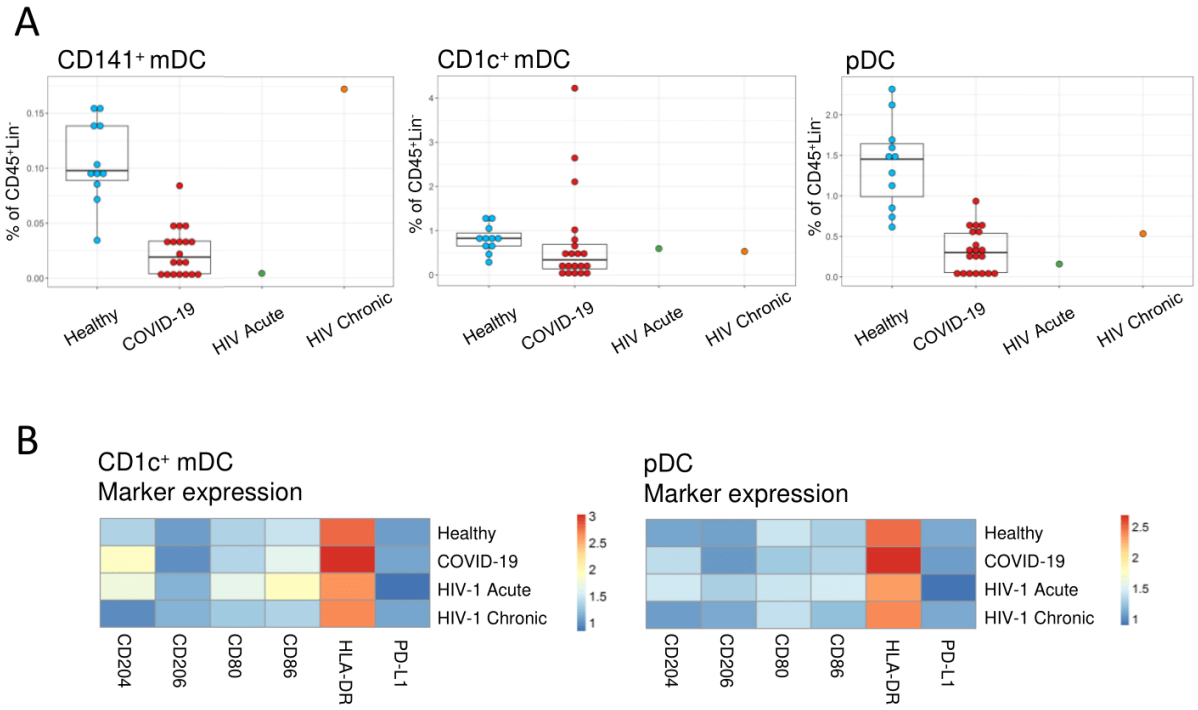

Figure 15 – **Circulating dendritic cells are altered in acute HIV-1 infection**.
(**A**) Boxplots showing the frequencies and the medians of the identified population. Each dot represents one subject. (**B**) Heatmap showing the expression of co-stimulatory and activation markers within CD1c+ mDCs and pDCs for the HIV-1 acute and untreated HIV-1 chronic patients, as well as the healthy control and COVID-19 groups. CD141+ mDC marker expression is not shown given the low number of events.

These data showed the existence of more pro-inflammatory or M1-like profile in the circulating monocytes of the acute HIV-1 infected patients, in contrast with the rise of the immunomodulatory or M2-like profile in the acute COVID-19 cohort. However, some similarities were observed, such as the depletion of several DC subsets and of the Slan$^+$ non-classical monocytes.

3.3. Spectral Flow Cytometry Panel for Ex-vivo Study of HIV−1 and HIV−2 infected patients

3.3.1. An expanded flow-cytometry panel to profile circulating monocyte and dendritic cell populations

The use of spectral flow cytometry allowed for the expansion of the number of markers used, improving the characterization of circulating monocytes and dendritic cells populations (**Table 2**). To explore the application of the panel in future ex-vivo studies of HIV infected patients, two chronic HIV-2 under ART and a healthy control whole blood samples were stained with the updated surface panel and with intracellular SAMHD-1 (**Table 5**). Both HIV-2 patients did not show signs of an ongoing inflammatory response, exhibiting normal levels of CRP, ferritin and IL-6. Despite this, there were noticeable changes in the counts of circulating leukocytes, namely in the lymphocytes. Patient A showed slight above normal $CD4^+$ T-cell counts while Patient B showed the opposite, with decreased $CD4^+$ T-cell counts. The reduction in CD4+ T-cells and the lower counts at ART start indicate a worse disease control for Patient B, despite being under ART for longer time.

Table 5 - **Clinical Data and Blood Work from chronic HIV-2 and a Health Control.**

	Patient A	Patient B	Healthy Control
Sex	Female	Male	Male
Age (years)	70	72	23
CRP (mg/dl)	0.36	0.15	ND
Ferritin (ng/ml)	119	146	ND
Interleukin 6 (pg/ml)	3.8	5	ND
Lymphocytes/ml	1963	989.4	ND
$CD4^+$ T /ml	1166	322	ND
$CD8^+$ T /ml	585	362	ND
CD4/CD8 ratio	1.99	0.89	ND
Neutrophils/ml	4017	3305	ND
Lymphocytes/neutrophils ratio	0.49	0.30	ND
Monocytes/ml	442	547	ND
Basophils/ml	39	31	ND
Eosinophils/ml	39	164	ND
$CD4^+$ counts at diagnosis/ml	>500	<200	NA
Treatment duration (years)	2	20	NA
HIV-2 Plasma Viral Load (RNA cps/ml)	ULoD	ULoD	NA

CRP: C reactive protein; PCT: procalcitonin; NA: Not Applicable; ND: Not Done; ULoD: Under Limits of dectection.

The gating strategy utilized with the new panel was similar the one described in page **24**, differing in the identification of the monocytes in the $CD1c^{-/low}$ cells by the expression of CD33 and CD86 instead of the expression of HLA-DR and CD86. The monocyte subsets are then defined by CD14 and CD16 expression: Classical monocytes ($CD14^{high}CD16^{-/low}$); Intermediate monocytes ($CD14^{high}CD16^{+}$); Non-classical monocytes ($CD14^{low/-}CD16^{+}$) (**Figure 16**).

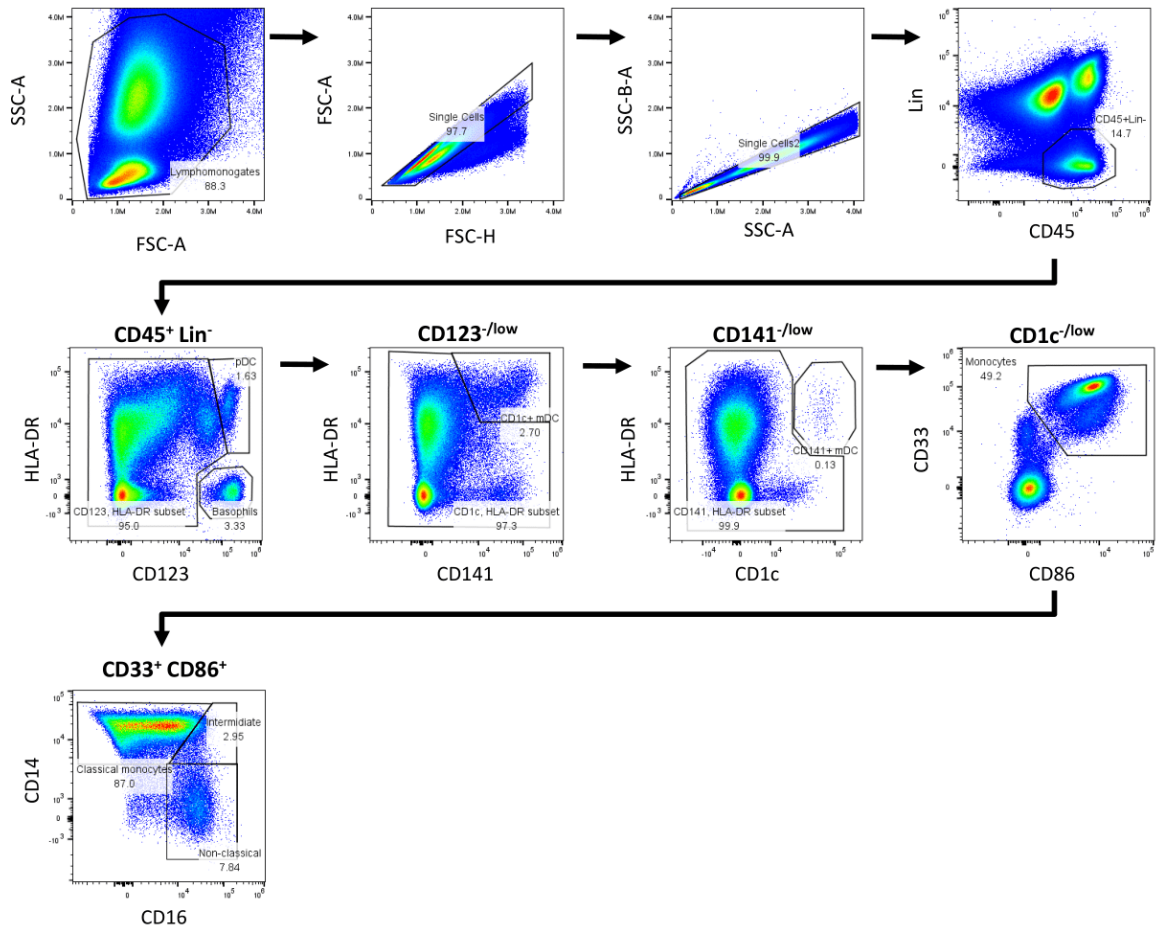

Figure 16 - **Gating strategy for profiling monocytes and DCs with a spectral flow cytometry panel**. Illustrative gating strategy used to identify monocytes and dendritic cells from whole blood, starting from 10 million leukocytes. Dot plots showing data from the healthy control.

An unsupervised analysis was performed on the $CD45^{+}Lin^{-}$ dataset by applying UMAP and then clustering with FlowSOM, resulting in 16 cluster (**Figure S3**). To facilitate interpretation, the clusters were then annotated into 10 subsets (**Figure 17A**) based on marker expression (**Figure 17B**).

The annotated subsets separated the main subsets of dendritic cells and monocytes. Regarding DC populations, it was possible to identify the pDC ($HLA{-}DR^{high}CD123^{+}$) and two subsets of mDCs, the $CD141^{+}$ ($HLA{-}DR^{high}CD141^{+}$) and $CD1c^{+}$ ($HLA{-}DR^{high}CD1c^{+}$). Basophil were identified as ($HLA\text{-}DR^{-}\ CD123^{+}$) subset.

Classical monocytes were defined by high CD14 expression, low or negative CD16 expression and positive CCR2 ($CD14^{high}\ CD16^{-/low}\ CCR2^{+}$), within classical monocytes it was possible to identify an additional subset that expressed the highest levels of CCR2, CD206 and CD16, as well as one of the highest of HLA-DR. Intermediate monocytes were identified by the expression of both CD14, CD16 and PD-L1, as well as the high expression of HLA–DR and low expression of both CCR2 and CX_3CR1 ($CD14^{+}\ CD16^{+}\ PD{-}L1^{+}\ CCR2^{low}\ CX_3CR1^{low}\ HLA{-}DR^{high}$). Finally, the non-classical monocyte subsets were classified by low to negative

expression of CD14 and positive CD16 expression. Non-classical monocytes also possessed the highest levels of CX_3CR1 and positive expression of PD–L1 ($CD14^{-/low}$ $CD16^{+}$ $PD–L1^{+}$ $CCR2^{-}$ CX_3CR1^{+} $HLA–DR^{low}$), the non-classical monocytes were then divided based of expression of Slan. Finally, the expression of SAMHD-1 varied among the subsets but as expected, monocytes all expressed high levels. Interestingly, non-classical monocytes expressed the highest levels of SAMHD-1 (**Figure S3** and **Figure 17B).**

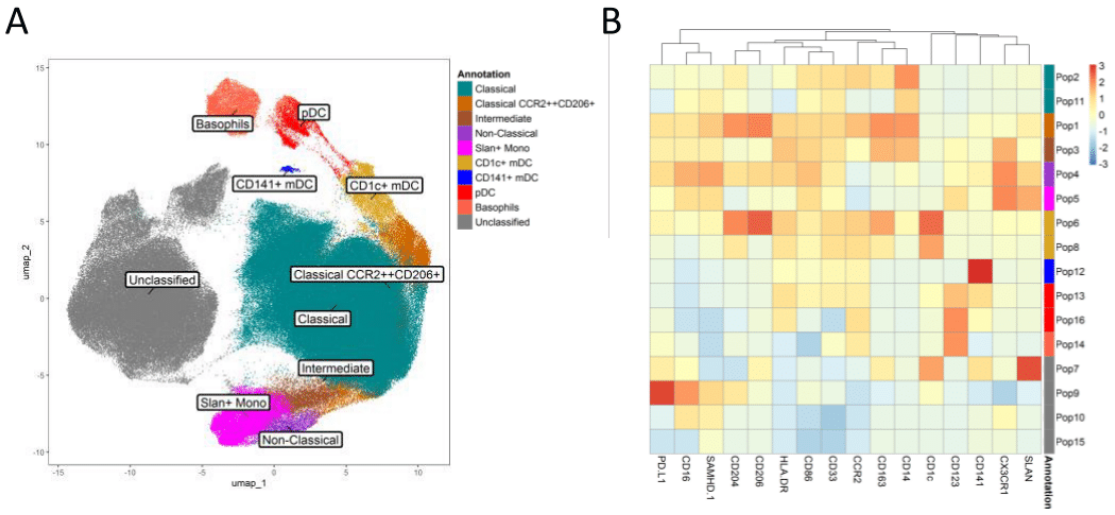

Figure 17 – **Circulating monocyte and DC profile in HIV-2 infection.**
(A) UMAP of the $CD45^{+}Lin^{-}$ dataset of all samples and **(B)** heatmap showing relative marker expression of the clusters obtained with the FlowSOM and subsequent manual annotation of the main subsets.

3.3.2. Phenotypic monocytes changes in chronic HIV-2 infected patients

Analysing relative subset distribution revealed that the subset $CCR2^{++}CD206^{++}$ of classical monocyte was almost exclusive to the HIV-2 infected patient A (**Figure 18A**), which also showed a decrease in Slan expressing non-classical monocytes. To confirm these observations, a manual gating analysis was performed in the monocyte compartments. Both HIV-2 patients showed an increased expression of CD16 in classical monocytes, which was more evident in the patient A (**Figure 18B**). Investigating the classical monocytes showed that in fact patient A exhibited a classical monocyte population expressing high levels of CCR2 and CD206 (**Figure 18C**).

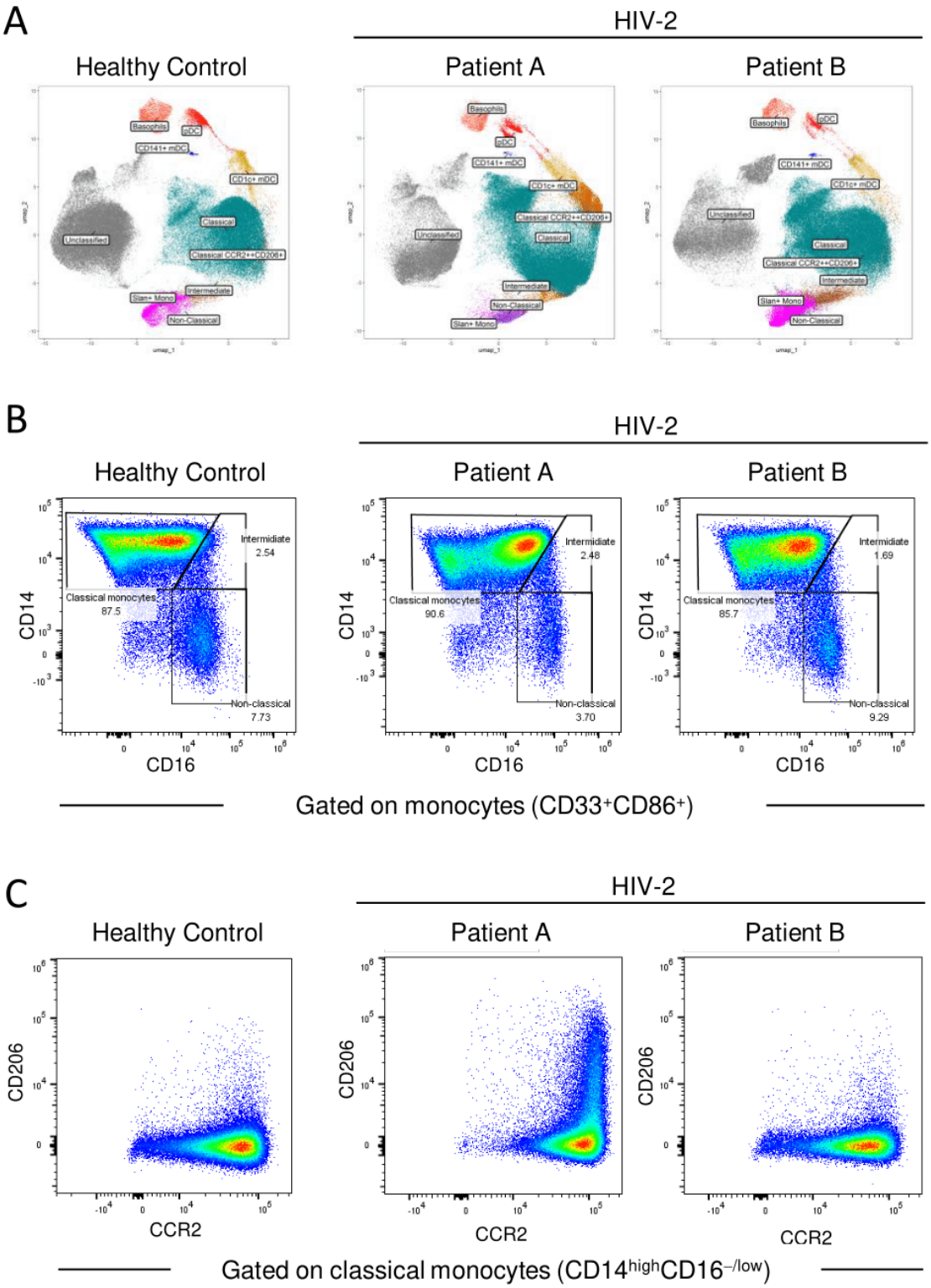

Figure 18 – **Classical monocyte phenotype in HIV-2 infection.**
(A) Relative subset distribution in both HIV-2 infected patients and the healthy control. **(B-C)** Dot plots of the manual analysis performed on all samples showing the expression of CD14 and CD16 in monocytes ($CD33^{+}CD86^{+}$) **(B)** and of CCR2 and CD206 in classical monocytes ($CD14^{high}\ CD16^{-/low}$) **(C)**.

4. Discussion

4.1. Severe COVID-19 recovery is linked to increased immunomodulatory phenotype in monocytes and dendritic cells

Characterizing the cell profile associated with the clinical COVID-19 recovery might be a potential tool to guide therapeutic approaches for the cure of critically ill SARS-CoV-2 infected patients. The longitudinal data presented showed that severe disease recovery was associated with the acquisition and expansion of an immunomodulatory profile characterized by the prevalence of an M2-like phenotype in circulating monocytes and dendritic cells.

Another notable feature observed in both ICU and No-ICU patients was the depletion of Slan$^+$ non-classical monocytes and dendritic cells. Several studies reported the decrease in non-classical monocytes in severe COVID-19 (Boechat *et al.*, 2021; Gatti *et al.*, 2020). Specifically, one study described a correlation between the decrease in Slan$^+$ cells with increased levels of soluble CD163 and CD14 in hospitalized COVID-19 patients (Zingaropoli *et al.*, 2021), However, in the last study cited, Slan+ cells were classified as DCs, despite in previous works, including genome wide profiling studies, Slan$^+$ cells were shown to cluster together with non-classical monocytes (Hofer *et al.*, 2019).

Non-classical monocyte depletion in severe Dengue virus infection was associated with increased activation and increased pro-inflammatory IL-6, IL-10 and IL-8 cytokines levels, leading to the hypothesis of a depletion caused by increased migration to tissues (Naranjo-Gómez *et al.*, 2019). Thus, the depletion of Slan+ monocytes and of the DCs populations observed could be due to increased migration to the tissues where they can contribute to the early inflammatory immune response. Interestingly, the low levels of these subsets were maintained until discharge, which could be due to the slow replenishing rate of Slan+ populations (Mager *et al.*, 2012). Another explanation might be increased cell death, as non-classical monocytes were shown to have increased inflammasome and pyroptotic cell death engagement upon SARS-CoV-2 infection (Ferreira *et al.*, 2021). Non-classical monocytes might be among the first to activate pyroptotic cell death mechanisms, given their pro-inflammatory profile and increased senescence (Ong *et al.*, 2018). However, pyroptosis seems unlikely as recent studies have shown that SARS-CoV-2 infection in monocytes inhibits the finalization of this process, leaving migration as the more likely answer (Ma *et al.*, 2021).

Interestingly, the patients from the studied cohort showed persistently low levels of the proinflammatory cytokines IL-1α, IL-1β, IFN–α2, IFN-γ and TNF-α. Several studies have demonstrated both *in-vitro* and *in-vivo* that SARS-CoV-2 infection inhibits IFN-α and IL-1β production (Blanco-Melo *et al.*, 2020; Ma *et al.*, 2021; Zhou *et al.*, 2020) and longitudinal studies have showed that the levels of IL-1β, IFN–α2, IFN-γ and TNF-α subside within the first days of infection (Haljasmägi *et al.*, 2020; Lucas *et al.*, 2020). The admission timepoint

evaluation of the present cohort might be representative of a later infection stage occurring after the decline of these cytokines, characterized by persistent systemic viral replication and high levels of inflammatory mediators.

The admission stage in the ICU patients' group was characterized by high levels of several proinflammatory cytokines such as IL-6 and IP-10, important inducer of the hyper-inflammatory syndrome, associated with worse prognosis in SARS-CoV-2 infection (Haljasmägi *et al.*, 2020) and other viral infections, such as H1N1 (Gao *et al.*, 2013).

The simultaneous development of an immune regulatory response was evident from the time of both hospital and ICU admission. The immunomodulatory profile was characterized by high levels of IL-10 and IL1-RA and the prevalence of circulating monocytes with a M2-like phenotype, expressing high levels of the scavenger receptors CD163, CD204 and CD206, a phenotype previously described in severe COVID-19 patients (Schulte-Schrepping *et al.*, 2020). Concordantly, SARS-CoV-2 infection of monocytes and macrophages *in vitro* seems to induce a M2-like profile by increasing IL-10 production (Boumaza *et al.*, 2021).

Regarding the ICU discharge stage, the M2-like phenotype was expanded and was accompanied by increased PD-L1 expression in classical monocytes displaying an M2-like phenotype. Simultaneously, at ICU discharge a decline of proinflammatory cytokines was observed, while significantly elevated levels of regulatory cytokines were still present.

The M2 phenotype might contribute to disease recovery, as M2 macrophages favour the non-inflammatory clearance of pathogens and cellular debris (Gordon e Martinez, 2010). On the other hand, the prevalence of an M1 profile and the associated damage caused by a sustained inflammatory response was associated by other authors with worsening of clinical symptoms in life-threatening viral infections (Cole *et al.*, 2017). The immune response in severe COVID–19 is characterized by a cytokine storm with defective IFN response, promoting extensive tissue damage and subsequent worsening of respiratory symptoms without effective pathogen elimination. The rise of a M2 phenotype might reduce the effects of the early rampant inflammation. Interestingly, steroids are among the very few effective treatments in severe COVID-19. Steroids are known to induce the M2 polarization in monocytes and macrophages, therefore, the favouring of this phenotype might be part of their therapeutic effect in severe COVID-19. (Sterne *et al.*, 2020).

Some limitations of this study should be mentioned, namely the relatively low sample size and the low number of female patients that made it impossible to assess the effect of the sex variable on the cellular phenotype However, it was not possible to exclude the impact of treatment in severe disease recovery, as it was not the purpose of the present study, and several severe patients were enrolled before routine steroid administration was implemented.

In conclusion, these results show the acquisition of an immunomodulatory profile at the recovery from severe COVID-19. Future studies with larger cohorts could possibly deepen this

analysis, evaluating the impact of therapeutic approaches in correlation with monocyte and dendritic cell phenotype. Also, the possible long-term consequences of the maintenance of an M2-like profile should be addressed. Finally, future therapeutic strategies directed to alter monocyte and DC phenotype might be helpful to improve the prognosis of patients that are experiencing the effects of severe infections associated with exacerbated inflammatory responses.

4.2. Acute HIV-1 infection is characterized by increased proinflammatory profile and Slan$^+$ monocyte depletion

The characterization of circulating monocytes and DCs profile in HIV-1 and SARS-CoV-2 acute infection highlighted the phenotypic plasticity of these cells, as seen by the different changes in the M1–M2-like profile balance in both infections. The M1-like phenotype was expanded in classical monocyte subset in the both the acute and chronic HIV-1 patients, contrasting with the M2-like shift observed in the acute SARS-Cov-2 infection.

Concerning the HIV-1 infected patients evaluated, a higher expansion of classical monocytes showing a M1-like profile was observed in the HIV-1 chronically infected ART naïve individual . Monocytes have been described to upregulated activation markers like HLA-DR during the sharp viremia peek observed in the acute stage of infection, such as in Fiebig stage II (Kazer *et al.*, 2020). Since these cells can stimulate the adaptive immune response with inflammatory cytokine production and antigen presentation, the increased presence of the M1-like phenotype might promote immune activation of CD4$^+$ T-cells, contributing to their depletion throughout HIV–1 infection (Sousa *et al.*, 2002). The pro-inflammatory state is known to persist even after ART and is thought to be a key factor in the higher incidence of non-AIDS co-morbidities in people living with HIV-1 (Bahrami *et al.*, 2016; Marcus *et al.*, 2020). This pro inflammatory response seen in early HIV-1 infection stages might contribute the dissemination of the virus (Ipp *et al.*, 2014).

Despite the differences observed in the phenotype of circulating cells in the HIV-1 versus the SARS-CoV-2 infected individuals, some similarities were observed, namely the depletion of the Slan$^+$ non-classical monocyte population in both acute viral infections. Non-classical monocytes produce inflammatory cytokines such as TNF-α, IL-1β and IL-12 and are highly mobile, quickly leaving the circulation to pass in the sites of inflammation (Anbazhagan *et al.*, 2014; Ancuta *et al.*, 2003). Specifically, the Slan$^+$ population is highly prolific in cytokine production, producing large amounts of TNF-α (Schäkel *et al.*, 2002). After leaving circulation, Slan$^+$ non-classical monocytes can adopt a DC-like phenotype and have been shown to possess the capacity to efficiently co-stimulate CD4$^+$ T-cells (Micheletti *et al.*, 2016; Schäkel *et al.*, 2006). Most studies on Slan$^+$ monocytes have been in the context of chronic inflammation, such as psoriasis, where these cells are found expanded (Hänsel *et al.*, 2011). The only reports of these cells in acute viral infection are our study on severe COVID-19 and another study that reported their depletion on COVID-19 patients (Zingaropoli *et al.*, 2021). The depletion seemed to be independent of age, since the acute HIV-1 patient here presented is younger that our SARS-CoV-2 infected patients and the same event was observed. In the context of acute HIV-1 infection, these cells might contribute to the viral set-point due to their

role as cytokine producers and ability to stimulate the $CD4^+$ T-cells, the main targets of HIV-1 infection. Interestingly, $Slan^+$ non-classical monocytes have a role during chronic stages of HIV-1 infection, being significantly expanded and responsible for the overproduction of TNF-α and IL-1β observed in viremic patients (Dutertre *et al.*, 2012; Tufa *et al.*, 2016). Coincidently, an expansion of $Slan^+$ monocytes was also reported in our chronic HIV-1 patient.

Finally, in accordance to existing literature (Grassi *et al.*, 1999; Zhou *et al.*, 2020), a contraction of circulating CD141+ mDCs and pDCs was reported in both acute infections, though a higher expression of the co-stimulatory ligands CD80 and CD86 was observed in the acute HIV-1 patient.

The early HIV-1 infection is mainly asymptomatic, makings the enrolment of patients in the acute stage rare. Due to this, a severe limitation is placed on this study sample size and these results should be corroborated by larger studies. Nevertheless, the previously undocumented depletion of the $Slan^+$ population hints at a possible role for these cells in acute viral infection pathogenesis and highlights circulating monocytes variable response to different infections. These results prompt the need for further investigation on $Slan^+$ monocytes in the context of acute viral responses and might help guide the design of new therapeutic strategies for the early disease stages.

4.3. Expanded spectral flow cytometry panel for the characterization of circulating monocytes and dendritic cell phenotype in patients chronically infected by HIV-2

Understating the factors that contribute to the differential course between HIV-1 and HIV−2 infections might unveil new aspects in HIV-1 pathogenesis. One major factor possibly contributing to the attenuated disease is the direct targeting of SAMHD-1 by the HIV-2. This restriction factor is expressed at high levels in monocytes, macrophages and dendritic cells (Laguette *et al.*, 2011). Thus, by targeting SAMHD-1, HIV-2 can infect more efficiently monocytes and DCs, which might be key in the different prognosis observed between the two infections.

Expanding the flow cytometry panel to take advantage of spectral flow cytometry technology allowed to better separate the non-monocyte and non-DC populations from the populations of interest. As such, it was possible to improve the definition of the major populations of circulating monocytes and dendritic cells, utilizing both unsupervised and supervised analysis of the data obtained. It was also possible to improve the characterization of each population phenotype in the context of HIV infection, by adding markers such as CCR2, CX_3CR1 and SAMHD-1.

To test the application of the new panel for *ex-vivo* studies in HIV-1 and HIV-2 infected patients, two chronic HIV-2 patients under ART and a healthy control whole blood samples were stained with the markers from the expanded panel. Both unsupervised and supervised analysis revealed different profiles among classical monocytes in the HIV-2 patients and interestingly also revealed differences among the two patients. The monocytes of both HIV-2 patients showed higher expression of CD16, to the point that most of the classical monocytes in these patients were positive for CD16, contrasting with the normal profile for circulating monocytes. The increased CD16 expression in monocytes has been previously described as resulting from chronic immune activation in both HIV-1 (Han *et al.*, 2009) and HIV-2 patients and correlating with levels sCD14 (Cavaleiro *et al.*, 2013). Increased expression of activation markers like CD16 reveal the chronic inflammation state that is thought to contribute to the higher incidence of co-morbidities in HIV-1 patients (Marcus *et al.*, 2020).

One marker that has been described as elevated in HIV-1 chronically infected individuals is CCR2, which can be used as rare co-receptor for HIV-1, but more interestingly its expression correlated with increased immune activation and to worse disease prognosis (Angela Covino, Sabbatucci e Fantuzzi, 2015; Williams *et al.*, 2014). In this study, the patient that showed the best disease control also showed a unique population displaying $CD14^{high}$ $CD16^{+}$ $CCR2^{high}$ $CD206^{+}$ $HLA{-}DR^{high}$. Interestingly, a similar

population was described in HIV-1 long term non-progressors (LTNP), those that maintain stable CD4+ counts for extended periods of time despite no ART (Prabhu *et al.*, 2019).

Hopefully future studies with larger cohort of chronic HIV-2, as well as chronic HIV-1 patients and age and sex matched healthy controls, utilizing this or a similar flow cytometry panel and measuring a wide array of cytokines or other soluble inflammatory mediators could corroborate these preliminary results.

Characterizing the phenotypic profiles in the attenuated HIV-2 infection might help to determine mechanisms for disease control in HIV-1. Identifying those mechanisms might lead to insights into both viruses' pathogenesis and guide therapeutics for the treatment of HIV-1.

5. References

ALCULUMBRE, Solana *et al.* - Plasmacytoid pre-dendritic cells (pDC): from molecular pathways to function and disease association. **Seminars in Cell and Developmental Biology**. . ISSN 10963634. 86:2019) 24–35. doi: 10.1016/j.semcdb.2018.02.014.

ALI, Nurshad - Elevated level of C-reactive protein may be an early marker to predict risk for severity of COVID-19. **Journal of Medical Virology**. . ISSN 10969071. 92:11 (2020) 2409–2411. doi: 10.1002/jmv.26097.

ANBAZHAGAN, Kolandaswamy *et al.* - Transcriptomic Network Support Distinct Roles of Classical and Non-Classical Monocytes in Human. **International Reviews of Immunology**. . ISSN 0883-0185. 33:6 (2014) 470–489. doi: 10.3109/08830185.2014.902453.

ANCUTA, Petronela *et al.* - Fractalkine preferentially mediates arrest and migration of CD16+ monocytes. **Journal of Experimental Medicine**. . ISSN 00221007. 197:12 (2003) 1701–1707. doi: 10.1084/jem.20022156.

ANGELA COVINO, Daniela; SABBATUCCI, Michela; FANTUZZI, Laura - The CCL2/CCR2 Axis in the Pathogenesis of HIV-1 Infection: A New Cellular Target for Therapy? **Current Drug Targets**. . ISSN 13894501. 17:1 (2015) 76–110. doi: 10.2174/1389450117011512171109 17.

AUFFRAY, Cedric *et al.* - Monitoring of blood vessels and tissues by a population of monocytes with patrolling behavior. **Science**. . ISSN 00368075. 317:5838 (2007) 666–670. doi: 10.1126/science.1142883.

AUFFRAY, Cedric; SIEWEKE, Michael H.; GEISSMANN, Frederic - Blood monocytes: Development, heterogeneity, and relationship with dendritic cells. **Annual Review of Immunology**. . ISSN 07320582. 27:2009) 669–692. doi: 10.1146/annurev.immunol.021908.132557.

AZEVEDO-PEREIRA, José Miguel; SANTOS-COSTA, Quirina - HIV Interaction With Human Host: HIV-2 As a Model of a Less Virulent Infection. **AIDS reviews**. . ISSN 1698-6997. 18:1 (2016) 44–53.

BACHEM, Annabell *et al.* - Superior antigen cross-presentation and XCR1 expression define human CD11c+CD141+ cells as homologues of mouse CD8+ dendritic cells. **Journal of Experimental Medicine**. . ISSN 1540-9538. 207:6 (2010) 1273–1281. doi: 10.1084/jem.20100348.

BAHRAMI, Hossein *et al.* - Inflammatory markers associated with subclinical coronary artery disease: The multicenter AIDS cohort study. **Journal of the American Heart Association**. . ISSN 20479980. 5:6 (2016). doi: 10.1161/JAHA.116.003371.

BIANCHINI, Mariaelvy *et al.* - PD-L1 expression on nonclassical monocytes reveals their origin and immunoregulatory function. **Science Immunology**. . ISSN 2470-9468. 4:36 (2019) eaar3054. doi: 10.1126/sciimmunol.aar3054.

BLANCO-MELO, Daniel *et al.* - Imbalanced Host Response to SARS-CoV-2 Drives Development of COVID-19. **Cell**. . ISSN 10974172. 181:5 (2020) 1036-1045.e9. doi: 10.1016/j.cell.2020.04.026.

BOECHAT, J. L. *et al.* - The immune response to SARS-CoV-2 and COVID-19 immunopathology – Current perspectives. **Pulmonology**. . ISSN 25310437. 2021). doi: 10.1016/j.pulmoe.2021.03.008.

BOUMAZA, Asma *et al.* - Monocytes and macrophages, targets of severe acute respiratory syndrome coronavirus 2: The clue for coronavirus disease 2019 immunoparalysis. **Journal of Infectious Diseases**. . ISSN 15376613. 224:3 (2021) 395–406. doi: 10.1093/infdis/jiab044.

CARVALHO, A. C. *et al.* - Population mobility and the changing epidemics of HIV-2 in Portugal. **HIV Medicine**. . ISSN 14642662. 13:4 (2012) 219–225. doi: 10.1111/j.1468-1293.2011.00963.x.

CAVALEIRO, Rita *et al.* - Monocyte and Myeloid Dendritic Cell Activation Occurs Throughout HIV Type 2 Infection, an Attenuated Form of HIV Disease. **The Journal of Infectious Diseases**. . ISSN 1537-6613. 207:11 (2013) 1730–1742. doi: 10.1093/infdis/jit085.

CHEN, Peng *et al.* - Perturbations of monocyte subsets and their association with T helper cell differentiation in acute and chronic HIV-1-infected patients. **Frontiers in Immunology**. . ISSN

16643224. 8:MAR (2017) 272. doi: 10.3389/fimmu.2017.00272.

CHIMEN, Myriam *et al.* - Monocyte Subsets Coregulate Inflammatory Responses by Integrated Signaling through TNF and IL-6 at the Endothelial Cell Interface. **The Journal of Immunology**. . ISSN 0022-1767. 198:7 (2017) 2834–2843. doi: 10.4049/jimmunol.1601281.

CIGNARELLA, Andrea *et al.* - The continuum of monocyte phenotypes: Experimental evidence and prognostic utility in assessing cardiovascular risk. **Journal of Leukocyte Biology**. . ISSN 19383673. 103:6 (2018) 1021–1028. doi: 10.1002/JLB.5RU1217-477RR.

COCKERHAM, Leslie R. *et al.* - CD4+ and CD8+ T cell activation are associated with HIV DNA in resting CD4+ T cells. **PLoS ONE**. . ISSN 19326203. 9:10 (2014). doi: 10.1371/journal.pone.0110731.

COLE, Suzanne L. *et al.* - M1-like monocytes are a major immunological determinant of severity in previously healthy adults with life-threatening influenza. **Journal of Clinical Investigation**. . ISSN 15588238. 2:7 (2017). doi: 10.1172/jci.insight.91868.

COSTA, Paola *et al.* - Differential disappearance of inhibitory natural killer cell receptors during HAART and possible impairment of HIV-1-specific CD8 cytotoxic T lymphocytes. **AIDS**. . ISSN 02699370. 15:8 (2001) 965–974. doi: 10.1097/00002030-200105250-00004.

COVINO, Daniela Angela *et al.* - Transcriptome Profiling of Human Monocyte-Derived Macrophages Upon CCL2 Neutralization Reveals an Association Between Activation of Innate Immune Pathways and Restriction of HIV-1 Gene Expression. **Frontiers in Immunology**. . ISSN 16643224. 11:2020). doi: 10.3389/fimmu.2020.02129.

CROZAT, Karine *et al.* - The XC chemokine receptor 1 is a conserved selective marker of mammalian cells homologous to mouse CD8α+ dendritic cells. **Journal of Experimental Medicine**. . ISSN 1540-9538. 207:6 (2010) 1283–1292. doi: 10.1084/jem.20100223.

DUTERTRE, Charles Antoine *et al.* - Pivotal role of M-DC8+ monocytes from viremic HIV-infected patients in TNFα overproduction in response to microbial products. **Blood**. . ISSN 00064971. 120:11 (2012) 2259–2268. doi: 10.1182/blood-2012-03-418681.

ELGUETA, Raul *et al.* - Molecular mechanism and function of CD40/CD40L engagement in the immune system. **Immunological Reviews**. . ISSN 01052896. 229:1 (2009) 152–172. doi: 10.1111/j.1600-065X.2009.00782.x.

FAJGENBAUM, David C.; JUNE, Carl H. - Cytokine Storm. **New England Journal of Medicine**. . ISSN 0028-4793. 383:23 (2020) 2255–2273. doi: 10.1056/NEJMra2026131.

FARIAS, Guilherme B. *et al.* - Acute HIV-1 and SARS-CoV-2 Infections Share Slan+ Monocyte Depletion—Evidence from an Hyperacute HIV-1 Case Report. **Viruses**. . ISSN 1999-4915. 13:9 (2021) 1805. doi: 10.3390/v13091805.

FERREIRA, André C. *et al.* - SARS-CoV-2 engages inflammasome and pyroptosis in human primary monocytes. **Cell Death Discovery**. . ISSN 2058-7716. 7:1 (2021) 43. doi: 10.1038/s41420-021-00428-w.

FIEBIG, Eberhard W. *et al.* - Dynamics of HIV viremia and antibody seroconversion in plasma donors. **AIDS**. . ISSN 0269-9370. 17:13 (2003) 1871–1879. doi: 10.1097/00002030-200309050-00005.

FIGUEIREDO-CAMPOS, Patrícia *et al.* - Seroprevalence of anti-SARS-CoV-2 antibodies in COVID-19 patients and healthy volunteers up to 6 months post disease onset. **European Journal of Immunology**. . ISSN 15214141. 50:12 (2020) 2025–2040. doi: 10.1002/eji.202048970.

GAO, Rongbao *et al.* - Cytokine and chemokine profiles in lung tissues from fatal cases of 2009 pandemic influenza A (H1N1): Role of the host immune response in pathogenesis. **American Journal of Pathology**. . ISSN 00029440. 183:4 (2013) 1258–1268. doi: 10.1016/j.ajpath.2013.06.023.

GASSEN, Sofie VAN *et al.* - FlowSOM: Using self-organizing maps for visualization and interpretation of cytometry data. **Cytometry Part A**. . ISSN 15524930. 87:7 (2015) 636–645. doi: 10.1002/cyto.a.22625.

References

GATTI, Arianna *et al.* - Decrease of Non-Classical and Intermediate Monocyte Subsets in Severe Acute SARS-CoV-2 Infection. **Cytometry Part A**. . ISSN 15524930. 97:9 (2020) 887–890. doi: 10.1002/cyto.a.24188.

GINHOUX, Florent; JUNG, Steffen - Monocytes and macrophages: Developmental pathways and tissue homeostasis. **Nature Reviews Immunology**. . ISSN 14741741. 14:6 (2014) 392–404. doi: 10.1038/nri3671.

GIRI, Malavika S. *et al.* - Circulating Monocytes in HIV-1-Infected Viremic Subjects Exhibit an Antiapoptosis Gene Signature and Virus- and Host-Mediated Apoptosis Resistance. **The Journal of Immunology**. . ISSN 0022-1767. 182:7 (2009) 4459–4470. doi: 10.4049/jimmunol.0801450.

GORDON, Siamon - Alternative activation of macrophages. **Nature Reviews Immunology**. . ISSN 14741733. 3:1 (2003) 23–35. doi: 10.1038/nri978.

GORDON, Siamon; MARTINEZ, Fernando O. - Alternative activation of macrophages: Mechanism and functions. **Immunity**. . ISSN 10747613. 32:5 (2010) 593–604. doi: 10.1016/j.immuni.2010.05.007.

GRASSI, Fernanda *et al.* - Depletion in blood CD11c-positive dendritic cells from HIV-infected patients. **AIDS**. . ISSN 0269-9370. 13:7 (1999) 759–766. doi: 10.1097/00002030-199905070-00004.

GREN, Susanne T. *et al.* - A Single-Cell Gene-Expression Profile Reveals Inter-Cellular Heterogeneity within Human Monocyte Subsets. **PLOS ONE**. . ISSN 1932-6203. 10:12 (2015) e0144351. doi: 10.1371/journal.pone.0144351.

GUAN, Wei-Jie *et al.* - Clinical Characteristics of Coronavirus Disease 2019 in China. **New England Journal of Medicine**. . ISSN 0028-4793. 382:18 (2020) 1708–1720. doi: 10.1056/nejmoa2002032.

HALJASMÄGI, Liis *et al.* - Longitudinal proteomic profiling reveals increased early inflammation and sustained apoptosis proteins in severe COVID-19. **Scientific Reports**. . ISSN 2045-2322. 10:1 (2020) 20533. doi: 10.1038/s41598-020-77525-w.

HAN, Junyan *et al.* - CD14highCD16+ rather than CD14lowCD16+ monocytes correlate with disease progression in chronic HIV-infected patients. **Journal of Acquired Immune Deficiency Syndromes**. . ISSN 15254135. 52:5 (2009) 553–559. doi: 10.1097/QAI.0b013e3181c1d4fe.

HÄNSEL, Anja *et al.* - Human slan (6-sulfo LacNAc) dendritic cells are inflammatory dermal dendritic cells in psoriasis and drive strong T 17/T 1 T-cell responses. **Journal of Allergy and Clinical Immunology**. . ISSN 00916749. 127:3 (2011) 787-794.e9. doi: 10.1016/j.jaci.2010.12.009.

HART, Derek N. J. - Dendritic Cells: Unique Leukocyte Populations Which Control the Primary Immune Response. **Blood**. . ISSN 1528-0020. 90:9 (1997) 3245–3287. doi: 10.1182/blood.V90.9.3245.

HOFER, Thomas P. *et al.* - 6-Sulfo LacNAc (Slan) as a Marker for Non-classical Monocytes. **Frontiers in Immunology**. . ISSN 16643224. 10:2019) 2052. doi: 10.3389/fimmu.2019.02052.

HUANG, Chaolin *et al.* - Clinical features of patients infected with 2019 novel coronavirus in Wuhan, China. **The Lancet**. . ISSN 1474547X. 395:10223 (2020) 497–506. doi: 10.1016/S0140-6736(20)30183-5.

HUBER, Wolfgang *et al.* - Orchestrating high-throughput genomic analysis with Bioconductor. **Nature Methods**. . ISSN 15487105. 12:2 (2015) 115–121. doi: 10.1038/nmeth.3252.

IPP, Hayley *et al.* - Role of inflammation in HIV-1 disease progression and prognosis. **Critical Reviews in Clinical Laboratory Sciences**. . ISSN 1549781X. 51:2 (2014) 98–111. doi: 10.3109/10408363.2013.865702.

JAIN, Vivek *et al.* - Antiretroviral therapy initiated within 6 months of HIV infection is associated with lower T-cell activation and smaller HIV reservoir size. **Journal of Infectious Diseases**. . ISSN 00221899. 208:8 (2013) 1202–1211. doi: 10.1093/infdis/jit311.

JONGBLOED, Sarah L. *et al.* - Human CD141+ (BDCA-3)+ dendritic cells (DCs) represent a unique myeloid DC subset that cross-presents necrotic cell antigens. **Journal of Experimental Medicine**. .

ISSN 1540-9538. 207:6 (2010) 1247–1260. doi: 10.1084/jem.20092140.

KAPELLOS, Theodore S. *et al.* - Human Monocyte Subsets and Phenotypes in Major Chronic Inflammatory Diseases. **Frontiers in Immunology**. . ISSN 1664-3224. 10:AUG (2019) 2035. doi: 10.3389/fimmu.2019.02035.

KAZER, Samuel W. *et al.* - Integrated single-cell analysis of multicellular immune dynamics during hyperacute HIV-1 infection. **Nature Medicine**. . ISSN 1546170X. 26:4 (2020) 511–518. doi: 10.1038/s41591-020-0799-2.

KRATZ, Mario *et al.* - Metabolic dysfunction drives a mechanistically distinct proinflammatory phenotype in adipose tissue macrophages. **Cell Metabolism**. . ISSN 19327420. 20:4 (2014) 614–625. doi: 10.1016/j.cmet.2014.08.010.

KUBOTA, Keigo *et al.* - CD163+CD204+ tumor-associated macrophages contribute to T cell regulation via interleukin-10 and PD-L1 production in oral squamous cell carcinoma. **Scientific Reports**. . ISSN 20452322. 7:1 (2017) 1–12. doi: 10.1038/s41598-017-01661-z.

LAGUETTE, Nadine *et al.* - SAMHD1 is the dendritic- and myeloid-cell-specific HIV-1 restriction factor counteracted by Vpx. **Nature**. . ISSN 0028-0836. 474:7353 (2011) 654–657. doi: 10.1038/nature10117.

LANDSMAN, Limor *et al.* - CX3CR1 is required for monocyte homeostasis and atherogenesis by promoting cell survival. **Blood**. . ISSN 0006-4971. 113:4 (2009) 963–972. doi: 10.1182/blood-2008-07-170787.

LÉCUROUX, Camille *et al.* - Identification of a particular HIV-specific CD8+ T-cell subset with a CD27+ CD45RO/RA+ phenotype and memory characteristics after initiation of HAART during acute primary HIV infection. **Blood**. . ISSN 00064971. 113:14 (2009) 3209–3217. doi: 10.1182/blood-2008-07-167601.

LEE, Jeong Seok *et al.* - Immunophenotyping of COVID-19 and influenza highlights the role of type I interferons in development of severe COVID-19. **Science Immunology**. . ISSN 2470-9468. 5:49 (2020) eabd1554. doi: 10.1126/sciimmunol.abd1554.

LI, Nan; ZHANG, Weiping; CAO, Xuetao - Identification of human homologue of mouse IFN-γ induced protein from human dendritic cells. **Immunology Letters**. . ISSN 01652478. 74:3 (2000) 221–224. doi: 10.1016/S0165-2478(00)00276-5.

LIU, Lifeng *et al.* - Foxp3+Helios+ regulatory T cells are associated with monocyte subsets and their PD-1 expression during acute HIV-1 infection. **BMC Immunology**. . ISSN 14712172. 20:1 (2019) 1–8. doi: 10.1186/s12865-019-0319-7.

LIU, Yong Jun - IPC: Professional type 1 interferon-producing cells and plasmacytoid dendritic cell precursors. **Annual Review of Immunology**. . ISSN 07320582. 23:2005) 275–306. doi: 10.1146/annurev.immunol.23.021704.115633.

LUCAS, Carolina *et al.* - Longitudinal analyses reveal immunological misfiring in severe COVID-19. **Nature**. . ISSN 14764687. 584:7821 (2020) 463–469. doi: 10.1038/s41586-020-2588-y.

MA, Juan *et al.* - SARS-CoV-2 nucleocapsid suppresses host pyroptosis by blocking Gasdermin D cleavage. **The EMBO Journal**. . ISSN 0261-4189. 40:18 (2021). doi: 10.15252/embj.2021108249.

MACDONALD, Kelli P. A. *et al.* - Characterization of human blood dendritic cell subsets. **Blood**. . ISSN 00064971. 100:13 (2002) 4512–4520. doi: 10.1182/blood-2001-11-0097.

MAGER, Konrad *et al.* - Reconstitution of 6-sulfo LacNAc dendritic cells after allogeneic stem-cell transplantation. **Transplantation**. . ISSN 15346080. 93:12 (2012) 1270–1275. doi: 10.1097/tp.0b013e31824fd8b4.

MARCUS, Julia L. *et al.* - Comparison of Overall and Comorbidity-Free Life Expectancy Between Insured Adults With and Without HIV Infection, 2000-2016. **JAMA network open**. . ISSN 25743805. 3:6 (2020) e207954. doi: 10.1001/jamanetworkopen.2020.7954.

MCINNES, Leland; HEALY, John; MELVILLE, James - UMAP: Uniform Manifold Approximation and

References

Projection for Dimension Reduction. **arXiv**. 2018).

MICHELETTI, Alessandra *et al.* - slan/M-DC8+ cells constitute a distinct subset of dendritic cells in human tonsils. **Oncotarget**. . ISSN 19492553. 7:1 (2016) 161–175. doi: 10.18632/ONCOTARGET.6660.

MOSSER, David M.; EDWARDS, Justin P. - Exploring the full spectrum of macrophage activation. **Nature Reviews Immunology**. . ISSN 14741733. 8:12 (2008) 958–969. doi: 10.1038/nri2448.

MUEMA, Daniel M. *et al.* - Association between the cytokine storm, immune cell dynamics, and viral replicative capacity in hyperacute HIV infection. **BMC Medicine**. . ISSN 17417015. 18:1 (2020) 1–17. doi: 10.1186/s12916-020-01529-6.

NARANJO-GÓMEZ, Juan S. *et al.* - Different phenotypes of non-classical monocytes associated with systemic inflammation, endothelial alteration and hepatic compromise in patients with dengue. **Immunology**. . ISSN 00192805. 156:2 (2019) 147–163. doi: 10.1111/imm.13011.

NAVEED, M. *et al.* - Review of potential risk groups for coronavirus disease 2019 (COVID-19). **New Microbes and New Infections**. . ISSN 20522975. 41:2021). doi: 10.1016/j.nmni.2021.100849.

NOVELLI, Sophie *et al.* - Persistence of monocyte activation under treatment in people followed since acute HIV-1 infection relative to participants at high or low risk of HIV infection. **EBioMedicine**. . ISSN 23523964. 62:2020). doi: 10.1016/j.ebiom.2020.103129.

O'BRIEN, Meagan; MANCHES, Olivier; BHARDWAJ, Nina - Plasmacytoid Dendritic Cells in HIV Infection. Em **Advances in experimental medicine and biology** [Em linha]. [S.l.] : Adv Exp Med Biol, 2012 [Consult. 4 out. 2021]. Disponível em WWW:<URL:https://pubmed.ncbi.nlm.nih.gov/22975872/>.v. 762. p. 71–107.

ONG, Siew-Min *et al.* - The pro-inflammatory phenotype of the human non-classical monocyte subset is attributed to senescence. **Cell Death & Disease**. . ISSN 2041-4889. 9:3 (2018) 266. doi: 10.1038/s41419-018-0327-1.

ONG, Siew-Min *et al.* - A Novel, Five-Marker Alternative to CD16–CD14 Gating to Identify the Three Human Monocyte Subsets. **Frontiers in Immunology**. . ISSN 1664-3224. 10:2019) 1761. doi: 10.3389/fimmu.2019.01761.

PATEL, Amit A. *et al.* - The fate and lifespan of human monocyte subsets in steady state and systemic inflammation. **Journal of Experimental Medicine**. . ISSN 15409538. 214:7 (2017) 1913–1923. doi: 10.1084/jem.20170355.

PICCOLO, Viviana *et al.* - Opposing macrophage polarization programs show extensive epigenomic and transcriptional cross-talk. **Nature Immunology**. . ISSN 15292916. 18:5 (2017) 530–540. doi: 10.1038/ni.3710.

PRABHU, Varsha M. *et al.* - Monocyte Based Correlates of Immune Activation and Viremia in HIV-Infected Long-Term Non-Progressors. **Frontiers in Immunology**. . ISSN 16643224. 10:2019). doi: 10.3389/fimmu.2019.02849.

ROGACEV, Kyrill S. *et al.* - Immunosuppression and monocyte subsets. **Nephrology Dialysis Transplantation**. . ISSN 14602385. 30:1 (2015) 143–153. doi: 10.1093/ndt/gfu315.

SAMUSIK, Nikolay *et al.* - Automated mapping of phenotype space with single-cell data. **Nature Methods**. . ISSN 15487105. 13:6 (2016) 493–496. doi: 10.1038/nmeth.3863.

SCHÄKEL, Knut *et al.* - 6-Sulfo LacNAc, a Novel Carbohydrate Modification of PSGL-1, Defines an Inflammatory Type of Human Dendritic Cells. **Immunity**. . ISSN 10747613. 17:3 (2002) 289–301. doi: 10.1016/S1074-7613(02)00393-X.

SCHÄKEL, Knut *et al.* - Human 6-Sulfo LacNAc-Expressing Dendritic Cells Are Principal Producers of Early Interleukin-12 and Are Controlled by Erythrocytes. **Immunity**. . ISSN 10747613. 24:6 (2006) 767–777. doi: 10.1016/j.immuni.2006.03.020.

SCHULTE-SCHREPPING, Jonas *et al.* - Severe COVID-19 Is Marked by a Dysregulated Myeloid Cell Compartment. **Cell**. . ISSN 00928674. 182:6 (2020) 1419-1440.e23. doi: 10.1016/j.cell.2020.08.001.

SCHULTZE, Joachim L.; ASCHENBRENNER, Anna C. - Systems immunology allows a new view on human dendritic cells. **Seminars in Cell and Developmental Biology**. . ISSN 10963634. 86:2019) 15–23. doi: 10.1016/j.semcdb.2018.02.017.

SILVIN, Aymeric *et al.* - Elevated calprotectin and abnormal myeloid cell subsets discriminate severe from mild COVID-19. **Cell**. . ISSN 00928674. 2020). doi: 10.1016/j.cell.2020.08.002.

SOUSA, Ana E. *et al.* - CD4 T Cell Depletion Is Linked Directly to Immune Activation in the Pathogenesis of HIV-1 and HIV-2 but Only Indirectly to the Viral Load. **The Journal of Immunology**. . ISSN 0022-1767. 169:6 (2002) 3400–3406. doi: 10.4049/jimmunol.169.6.3400.

STERNE, Jonathan A. C. *et al.* - Association between Administration of Systemic Corticosteroids and Mortality among Critically Ill Patients with COVID-19: A Meta-analysis. **JAMA - Journal of the American Medical Association**. . ISSN 15383598. 324:13 (2020) 1330–1341. doi: 10.1001/jama.2020.17023.

SUBAUSTE, C. S.; WAAL MALEFYT, R. DE; FUH, F. - Role of CD80 (B7.1) and CD86 (B7.2) in the immune response to an intracellular pathogen. **Journal of immunology**. . ISSN 0022-1767. 160:4 (1998) 1831–40.

TAK, Tamar *et al.* - Circulatory and maturation kinetics of human monocyte subsets in vivo. **Blood**. . ISSN 0006-4971. 130:12 (2017) 1474–1477. doi: 10.1182/blood-2017-03-771261.

THIEBLEMONT, Nathalie *et al.* - CD14lowCD16high: A cytokine-producing monocyte subset which expands during human immunodeficiency virus infection. **European Journal of Immunology**. . ISSN 00142980. 25:12 (1995) 3418–3424. doi: 10.1002/eji.1830251232.

THIESEN, Susanne *et al.* - CD14 hi HLA-DR dim macrophages, with a resemblance to classical blood monocytes, dominate inflamed mucosa in Crohnˈs disease. **Journal of Leukocyte Biology**. . ISSN 1938-3673. 95:3 (2014) 531–541. doi: 10.1189/jlb.0113021.

THOMAS, Katja *et al.* - Accumulation and therapeutic modulation of 6-sulfo LacNAc+ dendritic cells in multiple sclerosis. **Neurology: Neuroimmunology and NeuroInflammation**. . ISSN 23327812. 1:3 (2014). doi: 10.1212/NXI.0000000000000033.

TRIANT, Virginia A. *et al.* - Increased acute myocardial infarction rates and cardiovascular risk factors among patients with human immunodeficiency virus disease. **Journal of Clinical Endocrinology and Metabolism**. . ISSN 0021972X. 92:7 (2007) 2506–2512. doi: 10.1210/jc.2006-2190.

TROMBETTA, Amelia C. *et al.* - Severe COVID-19 Recovery Is Associated with Timely Acquisition of a Myeloid Cell Immune-Regulatory Phenotype. **Frontiers in Immunology**. . ISSN 1664-3224. 12:2021) 691725. doi: 10.3389/fimmu.2021.691725.

TUFA, Dejene M. *et al.* - Brief Report: HIV-1 Infection Results in Increased Frequency of Active and Inflammatory SlanDCs that Produce High Level of IL-1β. **JAIDS Journal of Acquired Immune Deficiency Syndromes**. . ISSN 1525-4135. 73:1 (2016) 34–38. doi: 10.1097/QAI.0000000000001082.

VALLE, Diane Marie DEL *et al.* - An inflammatory cytokine signature predicts COVID-19 severity and survival. **Nature Medicine**. . ISSN 1078-8956. 26:10 (2020) 1636–1643. doi: 10.1038/s41591-020-1051-9.

VANHEMS, Philippe *et al.* - Severity and prognosis of acute human immunodeficiency virus type 1 illness: A dose-response relationship. **Clinical Infectious Diseases**. . ISSN 10584838. 26:2 (1998) 323–329. doi: 10.1086/516289.

VARIN, Audrey *et al.* - Alternative activation of macrophages by IL-4 impairs phagocytosis of pathogens but potentiates microbial-induced signalling and cytokine secretion. **Blood**. . ISSN 00064971. 115:2 (2010) 353–362. doi: 10.1182/blood-2009-08-236711.

WILK, Aaron J. *et al.* - A single-cell atlas of the peripheral immune response to severe COVID-19. **medRxiv**. 2020) 2020.04.17.20069930. doi: 10.1101/2020.04.17.20069930.

WILLIAMS, Dionna W. *et al.* - CCR2 on CD14 + CD16 + monocytes is a biomarker of HIV-associated neurocognitive disorders. **Neurology - Neuroimmunology Neuroinflammation**. . ISSN 2332-7812.

1:3 (2014) e36. doi: 10.1212/NXI.0000000000000036.

WONG, Kok Loon *et al.* - Gene expression profiling reveals the defining features of the classical, intermediate, and nonclassical human monocyte subsets. **Blood**. . ISSN 0006-4971. 118:5 (2011) e16–e31. doi: 10.1182/blood-2010-12-326355.

XUE, Jia *et al.* - Transcriptome-Based Network Analysis Reveals a Spectrum Model of Human Macrophage Activation. **Immunity**. . ISSN 10747613. 40:2 (2014) 274–288. doi: 10.1016/j.immuni.2014.01.006.

ZAWADA, Adam M. *et al.* - Comparison of two different strategies for human monocyte subsets gating within the large-scale prospective CARE FOR HOMe Study. **Cytometry Part A**. . ISSN 15524922. 87:8 (2015) 750–758. doi: 10.1002/cyto.a.22703.

ZHANG, Dan *et al.* - Frontline Science: COVID-19 infection induces readily detectable morphologic and inflammation-related phenotypic changes in peripheral blood monocytes. **Journal of Leukocyte Biology**. . ISSN 19383673. 109:1 (2021) 13–22. doi: 10.1002/JLB.4HI0720-470R.

ZHOU, Runhong *et al.* - Acute SARS-CoV-2 Infection Impairs Dendritic Cell and T Cell Responses. **Immunity**. . ISSN 10974180. 53:4 (2020) 864-877.e5. doi: 10.1016/j.immuni.2020.07.026.

ZINGAROPOLI, Maria Antonella *et al.* - Increased sCD163 and sCD14 Plasmatic Levels and Depletion of Peripheral Blood Pro-Inflammatory Monocytes, Myeloid and Plasmacytoid Dendritic Cells in Patients With Severe COVID-19 Pneumonia. **Frontiers in Immunology**. . ISSN 1664-3224. 12:2021). doi: 10.3389/fimmu.2021.627548.

6. Supplementary

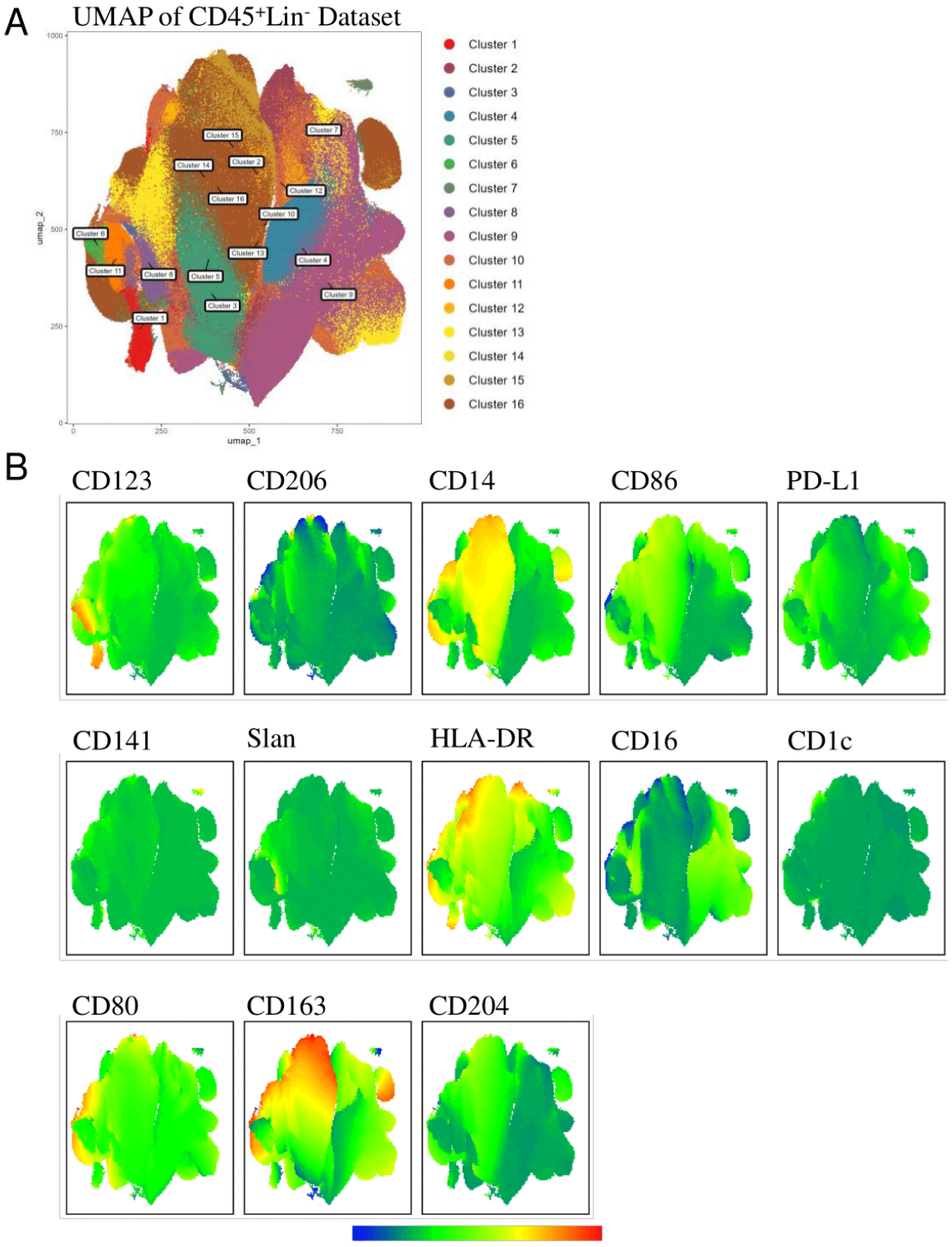

Figure S1 – **Unsupervised analysis of CD45^{+}Lin^{-} in COVID-19 Patients and Healthy Controls**. **(A)** UMAP of the CD45+Lin- dataset of all samples showing the 16 clusters obtained with X-Shift. **(B)** Marker expression within the UMAP.

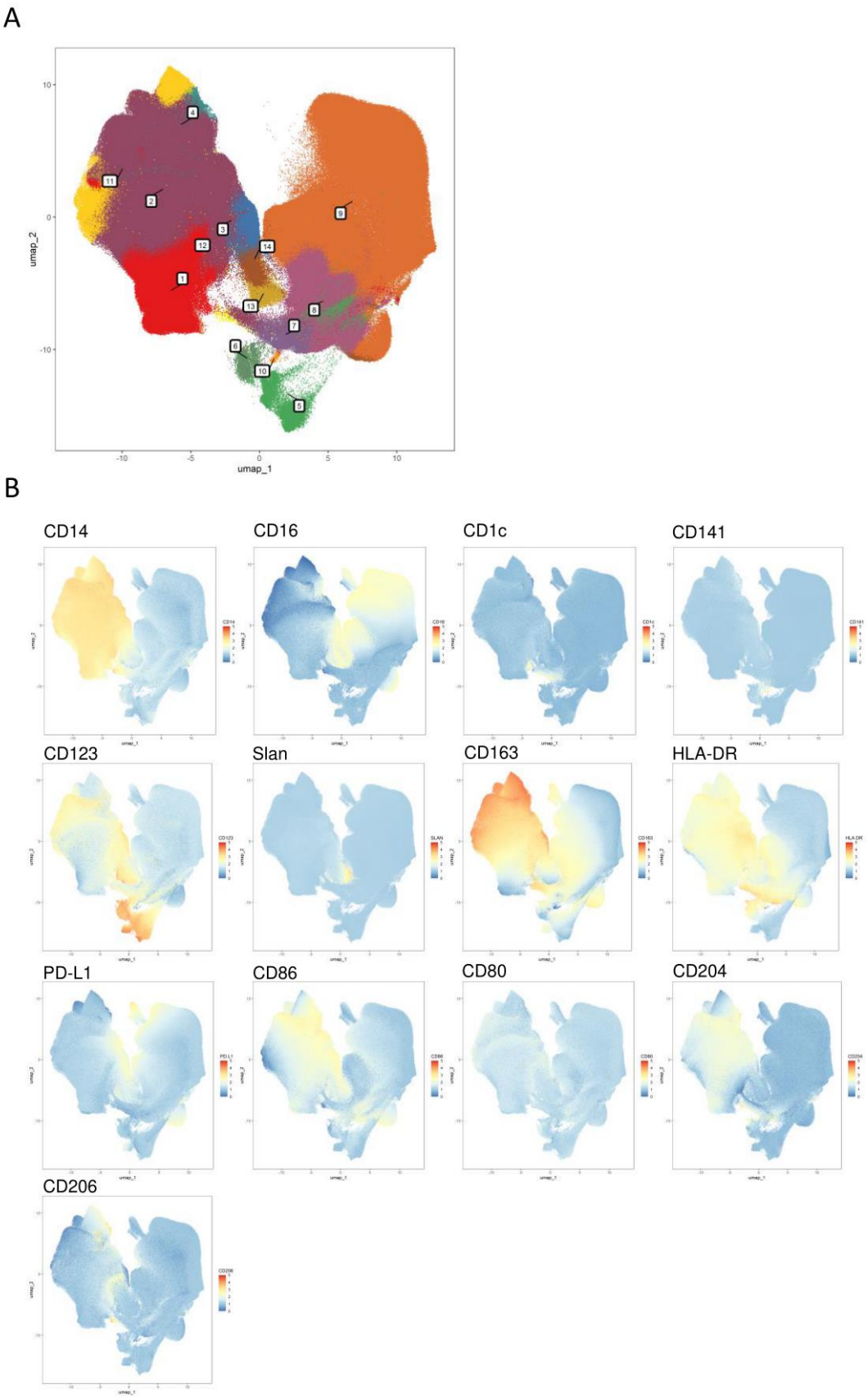

Figure S2 - **Unsupervised analysis of CD45^{+}Lin^{-} in acute HIV-1 and COVID-19 Patients and Healthy Controls**
(A) UMAP of the CD45+Lin- dataset of all samples showing the 14 clusters obtained with FlowSOM. **(B)** Marker expression within the UMAP.

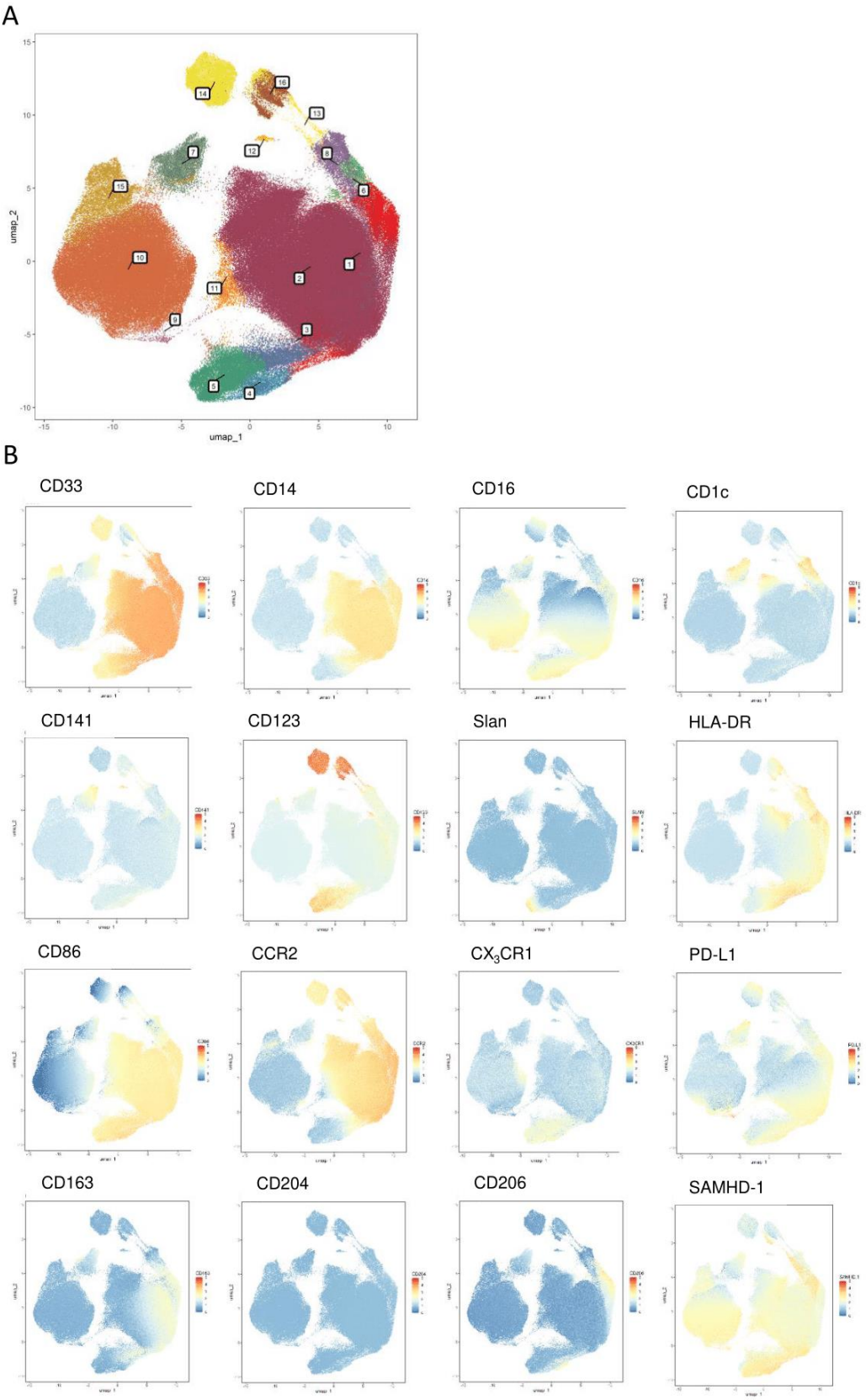

Figure S3 - **Unsupervised analysis of CD45^{+}Lin^{-} utilizing spectral flow cytometry panel.**
(A) UMAP of the CD45+Lin- dataset of all samples showing the 16 clusters obtained with FlowSOM.
(B) Marker expression within the UMAP.